Nicotinamide Phosphoribosyltransferase in Smooth Muscle Cells Maintains Genome Integrity, Resists Aortic Medial Degeneration, and Is Suppressed in Human Thoracic Aortic Aneurysm Disease

Alanna Watson, Zengxuan Nong, Hao Yin, Caroline O'Neil, Stephanie Fox, Brittany Balint, Linrui Guo, Oberdan Leo, Michael W.A. Chu, Robert Gros, J. Geoffrey Pickering

Rationale: **The thoracic aortic wall can degenerate over time with catastrophic consequences. Vascular smooth muscle cells (SMCs) can resist and repair artery damage, but their capacities decline with age and stress. Recently, cellular production of nicotinamide adenine dinucleotide (NAD^+) via nicotinamide phosphoribosyltransferase (Nampt) has emerged as a mediator of cell vitality. However, a role for Nampt in aortic SMCs in vivo is unknown.**

Objectives: **To determine whether a Nampt-NAD^+ control system exists within the aortic media and is required for aortic health.**

Methods and Results: **Ascending aortas from patients with dilated aortopathy were immunostained for NAMPT, revealing an inverse relationship between SMC NAMPT content and aortic diameter. To determine whether a Nampt-NAD^+ control system in SMCs impacts aortic integrity, mice with *Nampt*-deficient SMCs were generated. SMC-*Nampt* knockout mice were viable but with mildly dilated aortas that had a 43% reduction in NAD^+ in the media. Infusion of angiotensin II led to aortic medial hemorrhage and dissection. SMCs were not apoptotic but displayed senescence associated-ß-galactosidase activity and upregulated p16, indicating premature senescence. Furthermore, there was evidence for oxidized DNA lesions, double-strand DNA strand breaks, and pronounced susceptibility to single-strand breakage. This was linked to suppressed poly(ADP-ribose) polymerase-1 activity and was reversible on resupplying NAD^+ with nicotinamide riboside. Remarkably, we discovered unrepaired DNA strand breaks in SMCs within the human ascending aorta, which were specifically enriched in SMCs with low NAMPT. *NAMPT* promoter analysis revealed CpG hypermethylation within the dilated human thoracic aorta and in SMCs cultured from these tissues, which inversely correlated with *NAMPT* expression.**

Conclusions: **The aortic media depends on an intrinsic NAD^+ fueling system to protect against DNA damage and premature SMC senescence, with relevance to human thoracic aortopathy. (*Circ Res*. 2017;120:1889-1902. DOI: 10.1161/CIRCRESAHA.116.310022.)**

Key Words: aortic disease ■ cell aging ■ DNA damage ■ extracellular matrix

The aortic wall is subjected to unrelenting hemodynamic stress. Although structurally designed to withstand this stress, the aorta can nonetheless degenerate over time, particularly when also subjected to hypertension, atherosclerosis, or the effects of genetic mutations.[1,2] When the aorta degenerates, it dilates and becomes vulnerable to dissection and rupture. Vascular smooth muscle cells (SMCs) are important in maintaining aortic integrity, indicated by the development of thoracic aneurysms in individuals with mutations in SMC-specific genes.[3] SMC functions relevant to aortic homeostasis include contraction, synthesis of extracellular matrix, and the assembly of extracellular matrix fibers in accordance with local mechanical forces.[4,5] However, the abundance and functionality of SMCs can decline with age and chronic diseases.[1,6–8] Understanding the molecular pathways that can be engaged by SMCs to survive and retain their repertoire of functions in the stressed environment of the aortic wall may be critical to advancing strategies for reducing aortic catastrophes.

Editorial, see p 1849
In This Issue, see p 1843
Meet the First Author, see p 1844

Original received September 24, 2016; revision received March 25, 2017; accepted March 29, 2017. In February 2016, the average time from submission to first decision for all original research papers submitted to *Circulation Research* was 15.4 days.

From the Robarts Research Institute (A.W., Z.N., H.Y., C.O., R.G., J.G.P.), Division of Cardiology, Department of Medicine (J.G.P.), Department of Biochemistry (A.W., J.G.P.), Department of Medical Biophysics (B.B., J.G.P.), Department of Surgery (S.F., L.G., M.W.A.C.), and Department of Physiology and Pharmacology (R.G.), The University of Western Ontario, London Health Sciences Centre, Canada; and Department of Molecular Biology, Université Libre de Bruxelles, Gosselies, Belgium (O.L.).

The online-only Data Supplement is available with this article at http://circres.ahajournals.org/lookup/suppl/doi:10.1161/CIRCRESAHA.116.310022/-/DC1.

Correspondence to J. Geoffrey Pickering, MD, PhD, FRCPC, London Health Sciences Centre, 339 Windermere Rd, London, Ontario N6A 5A5, Canada. E-mail gpickering@robarts.ca

Novelty and Significance

What Is Known?

- The thoracic aorta can degenerate and dilate over time, predisposing to dissection and rupture.
- Vascular smooth muscle cells (SMCs) help maintain aortic integrity but their abundance and functionality can decline with age and disease.
- Nicotinamide phosphoribosyltransferase (NAMPT) is a key enzyme in nicotinamide adenine dinucleotide biosynthesis and has been found to slow SMC aging in vitro.

What New Information Does This Article Contribute?

- Nampt content is reduced in the aortic media of patients with dilated ascending aortopathy.
- SMC-specific knockout of *Nampt* in mice leads to senescence of SMCs in the aorta, accumulation DNA damage, aortic dilation, and angiotensin II–induced dissection.
- *NAMPT* promoter is hypermethylated, and unrepaired DNA breaks in medial SMCs were accumulated in human ascending aortopathy.

NAMPT is the rate-limiting enzyme for regenerating nicotinamide adenine dinucleotide in the cell. Its role in the vasculature is unknown. We generated mice with homozygous deficiency of Nampt in SMCs and found that loss of NAMPT rendered the aorta susceptible to medial hematomas and dissection. Interestingly, the aortas were marked by widespread SMC senescence and SMCs with unrepaired DNA damage. The activity of poly(ADP-ribose), a DNA repair enzyme that requires nicotinamide adenine dinucleotide supply, was prematurely exhausted in NAMPT-deficient SMCs. We also found that the aortas of patients with thoracic aortic aneurysms had lower levels of NAMPT compared with nondilated aortas. In addition, we detected unrepaired DNA strand breakage in SMCs within dilated human aortas, and this damage was particularly enriched in SMCs with the lowest NAMPT levels. Finally, we found that the *NAMPT* promoter was hypermethylated in the aortic media of aortopathy patients, pointing to epigenetic basis for compromised NAMPT production. Together, the results uncover an endogenous nicotinamide adenine dinucleotide–fueling system in the aortic media that protects against DNA damage and premature SMC senescence. These findings open a new perspective on the pathogenesis, and possible management, of human thoracic aneurysm disease.

Nonstandard Abbreviations and Acronyms	
Ang II	angiotensin II
NAD$^+$	nicotinamide adenine dinucleotide
Nampt	nicotinamide phosphoribosyltransferase
PAR	poly(ADP-ribose)
PARP1	poly(ADP-ribose) polymerase-1
SMC	smooth muscle cell

Nicotinamide adenine dinucleotide (NAD$^+$) is an essential dinucleotide that serves as a cofactor for the oxidation–reduction events of cellular nutrient metabolism. NAD$^+$ can also serve as a signaling nucleotide that regulates gene expression, genome integrity, and mitochondrial function. When NAD$^+$ participates in signaling reactions, it does so as an enzyme substrate rather than a cofactor and is, thus, consumed in the process. The most potent NAD$^+$-consuming reaction is believed to be the assembly of poly(ADP-ribose) (PAR) on histones, an event triggered by DNA strand breakage and catalyzed by the enzyme poly(ADP-ribose) polymerase-1 (PARP1).[9] Other NAD$^+$-consuming enzymes include those of the sirtuin family, which catalyze deacetylation and ADP-ribose transfer reactions, and CD38, which generates cyclic ADP ribose.[10]

The growing recognition of the importance of NAD$^+$-consuming reactions has heightened interest in understanding the pathways by which NAD$^+$ is generated and replenished. NAD$^+$ can be synthesized from dietary sources, but the routes to NAD$^+$ production are proving to be complex and tissue specific.[11] Important to maintaining the NAD$^+$ pool is the salvage pathway, wherein nicotinamide liberated during NAD$^+$-consuming reactions is recycled back to NAD$^+$.[10,12,13] Nicotinamide phosphoribosyltransferase (Nampt) is the rate-limiting enzyme for this salvage pathway, converting nicotinamide to nicotinamide mononucleotide.[12] Development of the mouse embryo cannot proceed without Nampt.[13] As well, gene-targeting strategies in mice have revealed a pattern of degenerative or aging-related tissue dysfunction when Nampt is perturbed, including in the liver, skeletal muscle, and brain.[14–16]

A role for Nampt in SMC-based vascular health is less clear, but the possibility has been raised. Nampt is expressed in cultured SMCs, and its content and activity decline during advanced SMC aging.[7,12] As well, Nampt has been found to regulate in vitro SMC longevity and migratory behavior.[7,17] There are also reports that exogenous delivery of Nampt impacts SMC contractile function, although with contradictory findings.[18] Nampt is expressed in periaortic adipose tissue,[19] and altering NAD$^+$ metabolism through the diet has been found to suppress age-related aortic dysfunction.[20] However, it remains unknown whether Nampt is needed for aortic health or whether a Nampt-based NAD$^+$ generation system exists within the aortic media. Understanding the requisite routes of NAD$^+$ supply to the aortic media could have important implications for strategies to prevent the severe medial degeneration that can occur in patients and the often-fatal consequences.

We have studied the expression of NAMPT in the aortic media of patients with life-threatening thoracic aortic dilation disease. In addition, we have investigated the role of Nampt in the aortic media by in vivo ablation of *Nampt* in SMCs in mice. Our findings reveal the existence of an intrinsic NAD$^+$-fueling system in the aortic media and its necessity for maintaining aortic integrity. The findings also establish the importance of Nampt in DNA repair and senescence resistance in the aortic media, and epigenetic events that could compromise NAD$^+$ homeostasis in human thoracic aortopathy.

Methods

A detailed description of methods is provided in the Online Data Supplement and includes information on generating *Nampt*-deficient mouse models, immunohistochemistry and RNA

quantification in human and mouse aortas, laser capture microscopy, NAD^+ measurement, blood pressure measurement, aortic wall morphometry, senescence-associated ß-galactosidase activity, cell culture, time-lapse microscopy, detection of DNA damage by Comet assay, assessment of DNA methylation, and statistical analyses.

Human Aorta Material

Human ascending aortic tissue was obtained from patients undergoing ascending aortic replacement, coronary bypass surgery, or cardiac transplantation, as approved by the Western University Research Ethics Board. Maximum aortic diameter was determined from contrast-enhanced computed tomographic scan or echocardiogram obtained before surgery and histological assessments were performed on the maximally dilated region.

Animal Experiments

Mouse experiments followed protocols approved by the Western University Animal Use Committee. We used a Cre/LoxP strategy to generate mice with a homozygous deficiency of *Nampt* specifically in SMCs using *Nampt*$^{flox/flox}$ mice[21] and smMHC (smooth muscle myosin heavy chain)-Cre/eGFP mice[22] (Jackson Laboratories). Mini-osmotic pumps (Alzet Model 2004; Durect Corp) were implanted subcutaneously for infusion with either saline or angiotensin II (Ang II; 1.44 mg/kg/d) for 7 or 28 days. PARP activity was inhibited by twice daily intraperitoneal injections of olaparib (50 mg/kg, AZD2281; Selleckchem) for 8 days, beginning 24 hours before implantation of saline or Ang II-loaded mini-pumps.

Results

Medial SMCs in Dilated Human Thoracic Aortas Have Reduced NAMPT

To determine whether NAMPT is expressed in SMCs of the human aorta, we evaluated ascending aortas surgically harvested from patients with dilated ascending aortopathy (n=20; mean age 58.4±16.4) and compared the findings with those of nondilated ascending aorta harvested from individuals undergoing heart transplantation or coronary artery bypass surgery (n=16; mean age 68.7±14.1). The mean aortic diameter of diseased aortas was 54.3±9.5 mm and that of control aortas was 31.1±2.8 mm (P<0.0001). Individual patient demographic data, aortic diameter, and aortic valve configuration and function are presented in Online Table I.

Immunostaining revealed widespread NAMPT expression in medial SMCs of the normal caliber aortas, with signal in both cytoplasm and nucleus (Figure 1A). Medial cell NAMPT expression was also evident in dilated aortas. However, the NAMPT signal was more heterogeneous and on average 34% lower (Figure 1B through 1D), as assessed by DAB (3,3′-diaminobenzidine) intensity analysis. Reduced NAMPT expression in the media of dilated aortas was also observed at the transcript level (Figure 1E). Interestingly, there was an inverse relationship between aortic medial NAMPT content and the maximal diameter of the ascending aorta (R^2=0.44; P<0.0001). This inverse relationship existed for both the entire patient cohort and only those patients with ascending aortopathy (R^2=0.31; P=0.009; Figure 1F) and persisted after adjusting for patient age (P=0.016). These findings implicate a NAMPT-based NAD^+ biosynthesis pathway within SMCs of the human aorta. Moreover, they suggest that this local biosynthetic machinery is related to aortic medial integrity.

Generation of Mice With SMC Nampt Gene Ablation

To determine whether Nampt within SMCs plays a role in aortic health, we generated mice with targeted deletion of *Nampt* in SMCs, using the smMHC-Cre/eGFP-expressing mouse line[22] and *Nampt*$^{flox/flox}$ mice.[21] Evaluation of eGFP in smMHC-Cre/eGFP mice confirmed Cre recombinase in the aorta, as assessed by whole organ microscopy and immunostaining (Online Figure I). Analysis of >200 offspring from a 2-step breeding protocol revealed close to expected Mendelian ratios for the predicted genotypes: 26.7% WT, 29.1% SMC-specific *Nampt* heterozygous, 20.6% *Nampt* heterozygous, and 23.5% SMC-*Nampt* knockout (KO).

Laser capture microdissection and quantitative reverse transcription-polymerase chain reaction revealed that *Nampt* transcript abundance in thoracic aortic media of SMC-*Nampt* KO mice was reduced to 13.5% that of control mice (Figure 2A). Immunostaining revealed nuclear and cytoplasmic Nampt protein in medial SMCs of control aortas, with the nuclear signal being stronger (Figure 2B). Nampt was undetectable in the aortic media of SMC-*Nampt* KO mice in all but rare cells but still detectable in endothelial cells and adventitial cells (Figure 2B). We also determined aortic NAD^+ content, using an NAD^+ cycling assay. This revealed a 43.2% reduction in NAD^+ content in SMC-*Nampt* compared with control mice (Figure 2C). Thus, *Nampt* is expressed in SMCs of the mouse aortic media and its depletion in SMCs, obtained using a Cre-lox approach, compromised aortic NAD^+ homeostasis.

Mice With SMC Nampt Deletion Have Modestly Dilated Thoracic Aortas

SMC-*Nampt* KO mice were viable and displayed no gross evidence of vascular anomalies. The average mean arterial pressure and heart rate of 8-week-old SMC-*Nampt* KO mice were not significantly different than those of control mice (Online Figure II). Immunostaining revealed abundant smooth muscle α-actin in medial SMCs, a normal number of lamellar units throughout the aorta, and unaltered medial SMC content (Figure 2E and 2F). Quantification of lumen area of aortas fixed at physiological pressure did, however, reveal modest dilation of the ascending and descending thoracic aortic regions (by 16.7% and 12.4%, Figure 2G). As well, the aortic medial areas of SMC-*Nampt* KO mice were mildly reduced in the ascending, descending thoracic, and suprarenal regions (by 13.2%, 17.0%, and 24.5%, respectively, Figure 2H). Transcript analysis revealed a modest (27.2%) decrease in mRNA abundance of SM-α-actin (P=0.001) and a 1.4-fold increase in *Mmp2* expression (P=0.005) with no change in *Timp1* expression (P=0.010).

Mice With SMC Nampt Deletion Are Susceptible to Ang II–Induced Aortic Dissection

To ascertain the response of the *Nampt*-deficient aorta to disease-associated stress, mice were subjected to continuous delivery of Ang II (1.44 mg/kg/d) by subcutaneous mini-pump. Interestingly, this was associated with a 54% decrease in aortic *Nampt* transcript abundance (P=0.009) and a concordant trend for NAD^+ content (P=0.063; Online Figure III). Mean arterial blood pressure increased at 7 days, with no significant

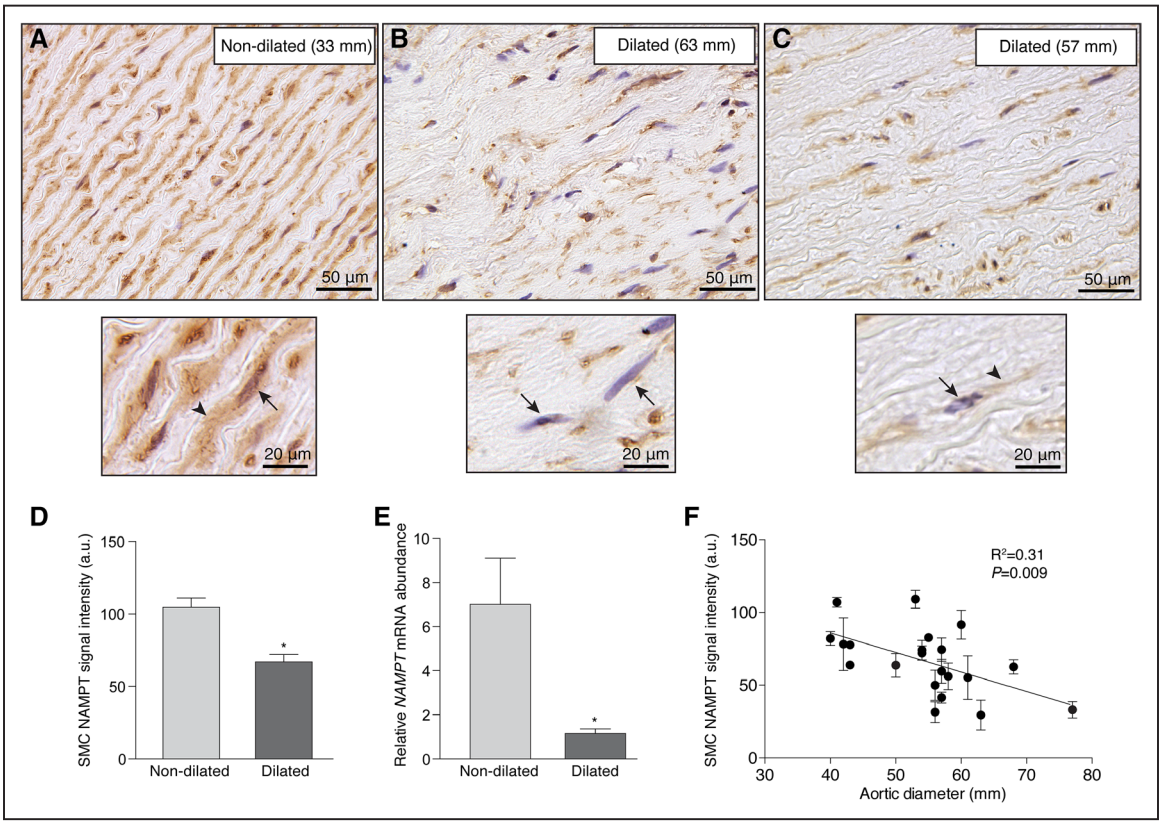

Figure 1. Human ascending aortic dilation is associated with reduced nicotinamide phosphoribosyltransferase (NAMPT). A and **B**, Photomicrographs of paraformaldehyde-fixed nondilated (**A**) and dilated (**B** and **C**) human aorta sections immunostained for NAMPT and counterstained with hematoxylin. Arrow in zoomed image of (**A**) depicts nuclear signal, and arrowhead depicts cytoplasmic signal. Arrows in zoomed image of (**B**) indicate NAMPT-negative cells. Arrow in zoomed image of (**C**) indicates absent nuclear signal, and arrowhead depicts weak cytoplasmic signal. **D.** Graph depicting NAMPT content in aortas from patients with control, nondilated aortas (n=16) and dilated aortas (n=20). **P*<0.0001 **E**, Graph depicting *NAMPT* mRNA abundance in control (n=6) and dilated (n=6) aortas. **P*=0.038 **F**, Inverse relationship between NAMPT content in dilated aortas and aortic diameter (n=20).

differences among the groups (25.3±4.3, 16.5±18.0, and 34.5±22.3 mm Hg for WT control, *Nampt* heterozygous control, and SMC-*Nampt* KO, respectively; *P*=0.285). However, there was striking aortic hemorrhage in SMC-*Nampt* KO mice, evident microscopically and grossly. Half of the mice displayed aortic hematomas after 7 days, and this increased to 62.5% on day 28. The hemorrhage typically was within the outer 1 or 2 medial layers and could be extensive, with local elastin breakage (Figure 3A). The hematomas did not rupture into the adventitia, as typically seen in Ang II–infused atherosclerotic mice, but instead could be found at multiple sites and dissecting along the length of the aortic media. In contrast, there was no grossly detectable hemorrhage in control mice subjected to Ang II, although microscopic hemorrhage in the ascending aorta was found in 24% of mice. These small bleeds, also noted in other reports,[23] had resolved by 28 days of Ang II delivery (Online Table II). A similar profile was observed for *Nampt* heterozygous mice (14% microscopic hemorrhage in the ascending aorta). Transcript analysis of whole aortas revealed that SM-α-actin expression was 22.2% lower in Ang II–infused SMC-*Nampt* KO than Ang II–infused control mice (*P*=0.0001), and expression of *Col1a1* was 37.4% lower (*P*=0.002). However, the *Mmp2/Timp1* ratio did not increase and in fact reduced somewhat (20.9%; *P*=0.002). Immunostaining for CD45 showed no differences between control and SMC-KO mice before or after Ang II infusion (data not shown).

Because of a trend toward greater Ang II–induced blood pressure response in SMC-*Nampt* KO mice, we determined whether blood pressure elevation, in and of itself, might be responsible for the more striking aortic disruption. For this, control mice were subjected to double infusion of phenylephrine and Ang II, which elevated the mean arterial pressure by 37.2±16.4 mm Hg. This increase was associated with only localized hemorrhage confined to the ascending aorta in 25% of mice (n=8), a profile not different than that of control mice subjected to Ang II. Collectively, these findings reveal that aortas in SMC-*Nampt* KO mice are prone to Ang II–induced disruption by hematoma and dissection, with minor changes in expression of SM-α-actin and type I collagen chains. Furthermore, whereas control mice adapted over 28 days to the disrupting potential of Ang II, SMC-*Nampt* KO mice remained vulnerable.

Ang II–Induced Cell Loss in Mice With SMC-Nampt KO Mice

Twenty-eight days of Ang II infusion in control mice resulted in a 1.8-fold increase in medial SMC content in the ascending aorta (Figure 3B and 3C) but no change in SMC content in the descending thoracic aorta, confirming a site-specific response that has been previously noted.[24] In

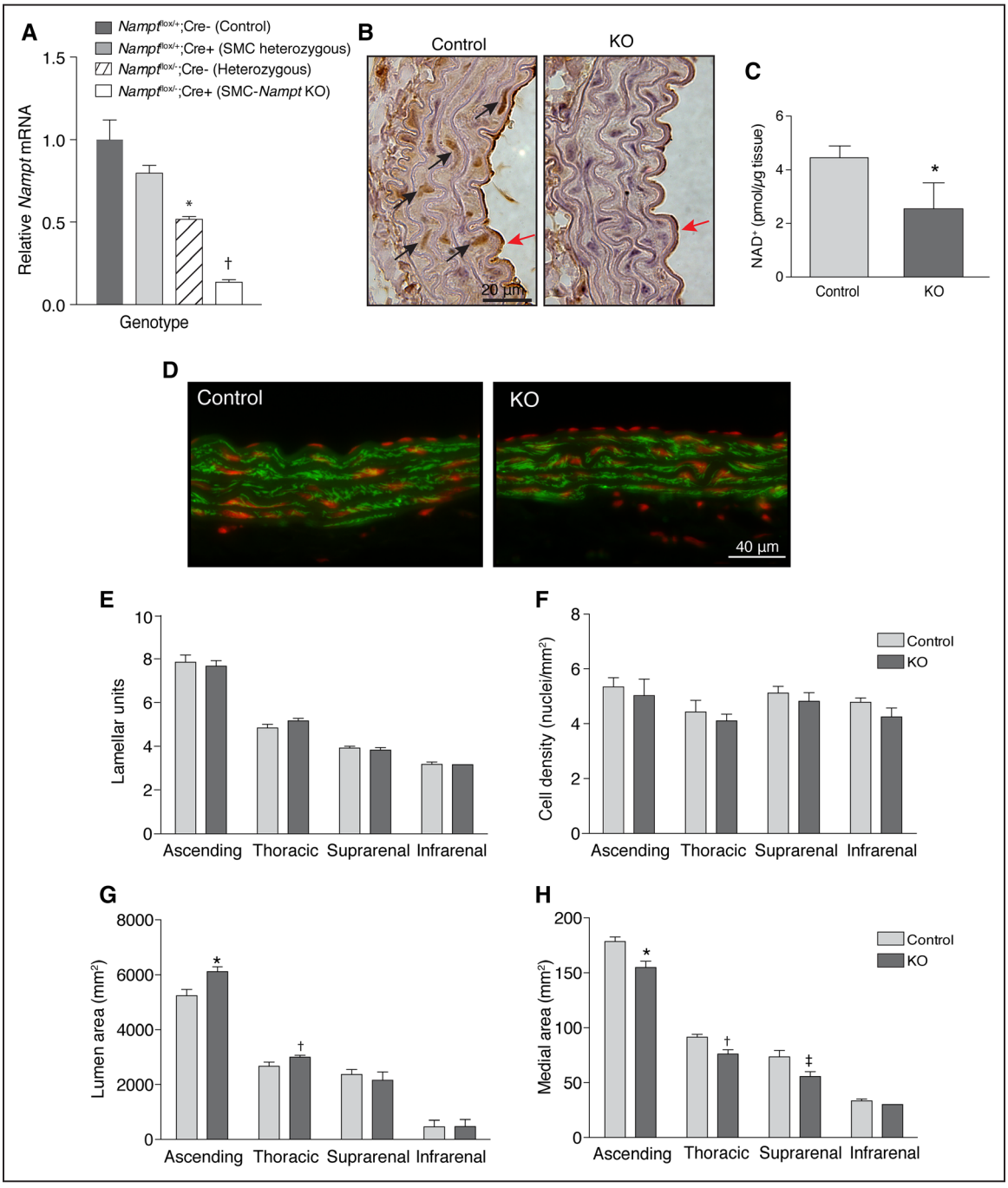

Figure 2. Deletion of nicotinamide phosphoribosyltransferase (*Nampt*) in smooth muscle cells (SMCs) in mice yields modest aortic dilatation. A, Graph depicting *Nampt* transcript abundance in the mouse aortic media harvested using laser capture microdissection, measured by quantitative reverse transcription-polymerase chain reaction. Medial tissues from 3 mice for each genotype were studied. **P*=0.0034 vs control, †*P*<0.0001 vs control **B**, Photomicrographs of thoracic aortic sections from control and SMC-*Nampt* knockout (KO) mice, immunostained for Nampt. Black arrows depict Nampt expression in SMCs, and red arrows depict Nampt expression in endothelial cells. **C**, Graph of nicotinamide adenine dinucleotide (NAD^+) content in acidic extracts of endothelium-denuded aortas of control and SMC-Nampt KO mice. **P*=0.024 vs control. **D**, Sections from the descending thoracic aorta of 12-wk-old mice stained for smooth muscle α-actin (green) and propidium iodide (red). **E–H**, Graphs showing the number of elastic lamellae per regional cross section (**E**), medial cell density (**F**), regional aortic lumen area (**G**), and medial area (**H**). **P*=0.023 and †*P*=0.029 vs respective lumen area in control aortas, **P*=0.029, †*P*=0.004, and ‡*P*=0.027 vs respective medial area in control aortas.

contrast, in SMC-*Nampt* KO mice, medial SMC content in the ascending aorta did not increase in response to Ang II and in the descending thoracic aorta SMC content actually fell by 25.2% (Figure 3D). These aberrant responses occurred despite evidence for residual SMC proliferation in Ang II–infused SMC-*Nampt* KO mice, as indicated by Ki67 immunostaining (Online Figure IV), supporting a turnover profile skewed toward cell loss. This loss of SMCs was evident both as scattered SMC dropout and cell-free foci of proteoglycan-rich matrix (Figure 3E). Cell-poor zones were

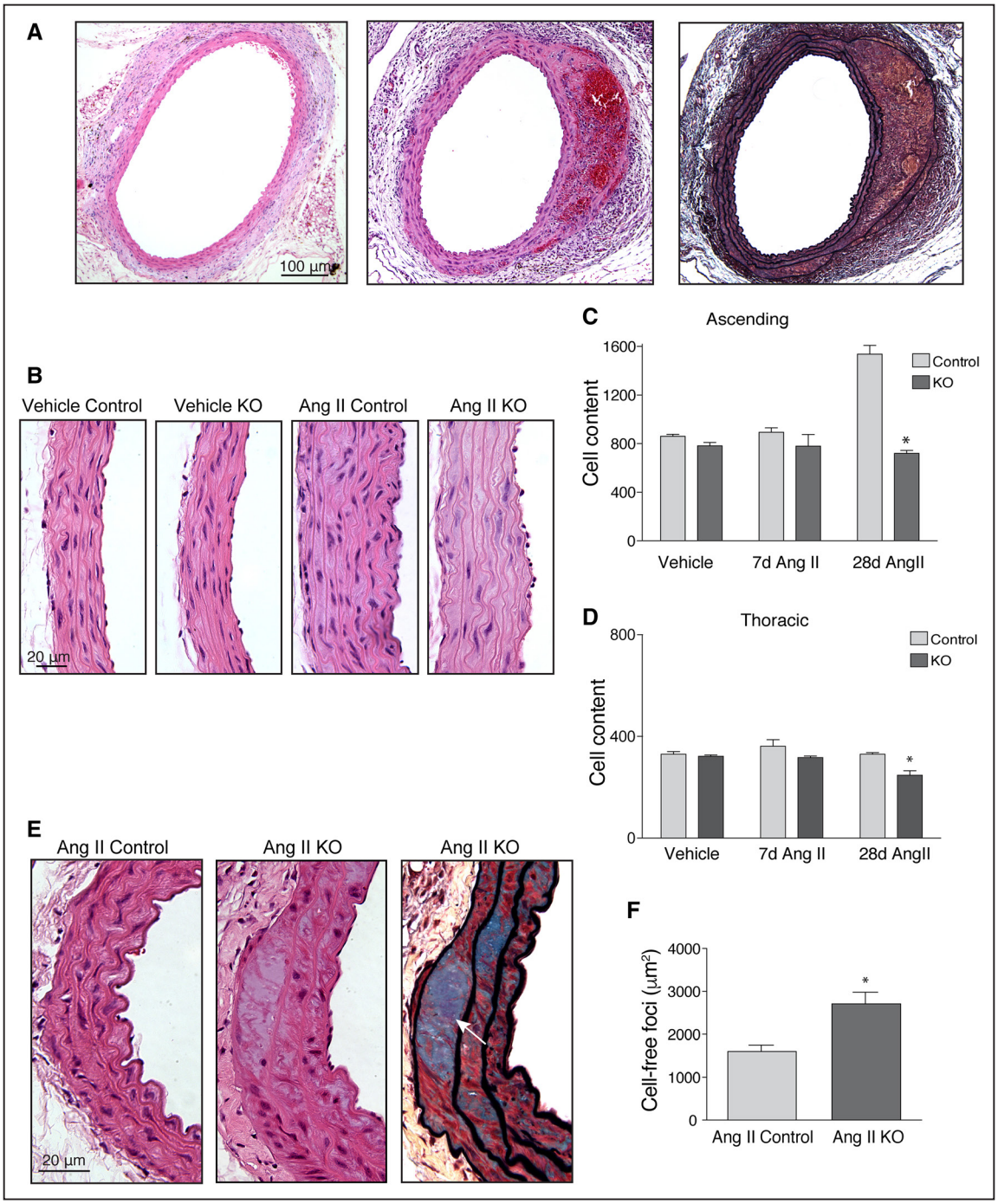

Figure 3. Smooth muscle cell (SMC)-nicotinamide phosphoribosyltransferase (*Nampt*) knockout (KO) mice are susceptible to aortic wall degeneration and dissection. A, Light micrographs of sections of the descending thoracic aorta of a control (**left**) and SMC-*Nampt* KO (**middle**) mouse after 28 d of infusion with angiotensin II (Ang II), stained with hematoxylin and eosin. **Right**: An adjacent section of the KO aorta stained with elastin trichrome, showing confinement of hemorrhage to the aortic media. **B**, Photomicrographs of sections of the ascending aorta stained with hematoxylin and eosin from vehicle-infused and Ang II–infused (28 d) control and SMC-*Nampt* KO mice. **C** and **D**, Graphs depicting cell content of the media cross section after Ang II infusion in ascending (**C**), **P*<0.0001 vs control, and descending thoracic (**D**) aortas **P*=0.002 vs control. **E**, Sections of descending thoracic aorta from control (**left**) and SMC-*Nampt* KO (**middle** and **right**) mice after 28 d of infusion with Ang II illustrating focal cell loss. **Right**: An adjacent section to that in the middle and stained with Movat pentachrome. Arrow depicts proteoglycan-rich cell-poor zone. **F**, Graph depicts the area of focal zones of SMC loss in the thoracic aorta, **P*=0.0003 vs control.

occasionally observed in control aortas subjected to Ang II but were 70% larger in aortas of SMC-*Nampt* KO mice (Figure 3F). Thus *Nampt*-depleted SMCs failed to adaptively fortify the ascending aorta and repopulate damaged regions in the descending aorta.

SMCs Within the Aorta of SMC-Nampt KO Mice Are Susceptible to Stress-Induced Premature Senescence

To determine whether the aberrant SMC responses to Ang II were caused by induction of apoptosis, aortas were evaluated

using TUNEL (terminal deoxynucleotide transferase-mediated dUTP nick end labeling) and active caspase-3 immunostaining. Surprisingly, although Ang II–induced apoptosis was evident in adventitial cells, we did not identify apoptosis signals in the thoracic aortic media (ascending or descending) of either control or *Nampt*-deficient mice (Online Figure V). We next asked whether SMCs instead developed features of senescence, recognizing that in vitro studies have implicated Nampt in slowing SMC aging.[7] Intravenous infusion and ex vivo immersion in X-Gal solution[25] revealed no senescence-associated ß-galactosidase activity in the aorta of control mice subjected to Ang II. Remarkably, however, in SMC-*Nampt*–deficient mice, there was senescence-associated ß-galactosidase activity throughout the ascending aorta, arch, and proximal descending thoracic aorta after 7 days of Ang II infusion (Figure 4A). Microscopy established that senescence-associated ß-galactosidase activity was confined to the medial layers of the aorta and particularly the outer medial layers (Figure 4B).

As an additional test for cell senescence, we immunostained aortic sections for the cell cycle inhibitor, $p16^{INK4a}$. This revealed a 6.1-fold increase in the abundance of p16-expressing

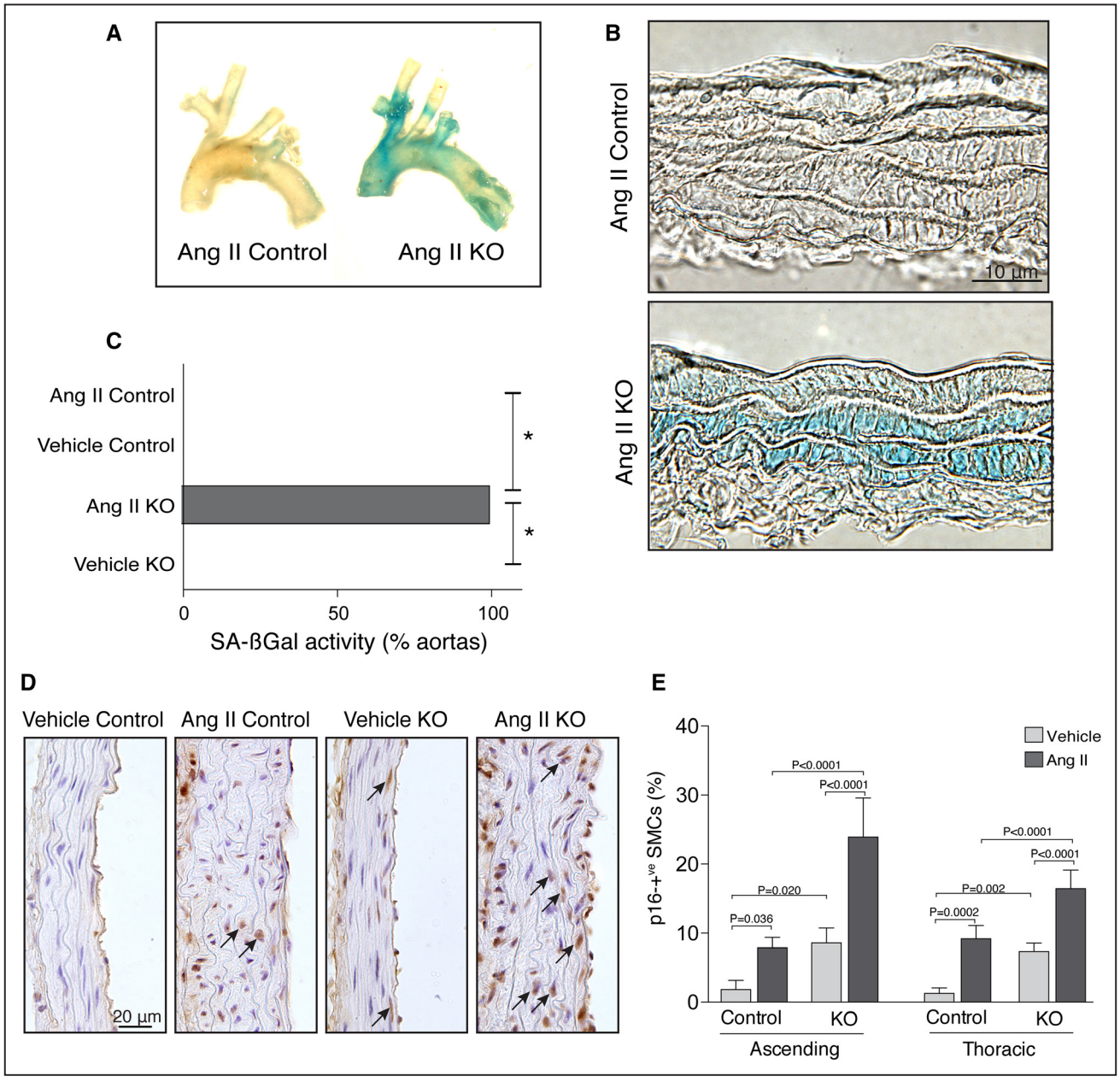

Figure 4. Nicotinamide phosphoribosyltransferase (*Nampt*)–deficient smooth muscle cells (SMCs) within the aorta undergo senescence cellular senescence in response to angiotensin II (Ang II) infusion. A, Whole mount images of ascending, arch, and proximal descending thoracic aortas harvested after 7 d of Ang II infusion and stained for senescence-associated β-galactosidase (SA-ßGal) activity (**blue**). **B**, Cryosections of the ascending aorta depicting SA-ßGal activity localized to the aortic media. **C**, Chart showing proportion of aortas (n=16) with SA-ßGal activity. *P=0.0011 **D**, Micrographs of ascending aorta subjected to 7 d of vehicle or Ang II infusion and immunostained for p16. Arrows depict p16-postive nuclei. **E**, Graph depicting prevalence of p16-positive nuclei.

cells in the media of the ascending aorta of Ang II–infused SMC-*Nampt* KO mice relative to Ang II–infused control mice and a 4.7-fold increase in the thoracic aorta (Figure 4E). Therefore, *Nampt* deficiency impacts the fate of SMCs in the aorta, whereby Ang II sends them into a state of premature senescence.

Nampt-Deficient SMCs Accumulate Oxidized DNA Lesions and Single-Stranded DNA Breaks

To explore why *Nampt*-ablated SMCs were prone to senescence, we assessed for DNA integrity. We first immunostained for the oxidized nucleoside, 8-oxo-2′-deoxyguanosine (8-oxodG), recognizing that reactive oxygen species can drive cell senescence.[26] The proportion of ascending aorta medial SMCs with oxidized DNA was 3-fold higher in SMC-*Nampt* KO mice than in control mice. After a 7-day infusion of Ang II, DNA oxidation in SMC-*Nampt* KO aortas was even more prevalent and was 2.5-fold greater than that in Ang II–infused control mice (Figure 5A and 5B). The oxidized DNA profile for SMCs in the thoracic aorta was similar although less striking (Figure 5B).

We next asked whether *Nampt*-deficient SMCs accumulated overt breaks in the DNA. For this, we established a culture system that enabled us to time the ablation of *Nampt* and evaluate different DNA break pressures. SMCs were cultured from aortas of *Nampt*$^{flox/flox}$ mice expressing Cre recombinase under the control of a tamoxifen-inducible promoter (Cre-ERT2). We then evaluated electrophoretic migration of cleaved DNA out of harvested nucleoids (Comet assay) after delivery of vehicle or hydroxytamoxifen. The latter induced robust *Nampt* knockdown (Online Figure IV). Interestingly, there was evidence for cleaved DNA in *Nampt*-ablated SMCs under baseline culture conditions (Figure 5C and 5D). Incubation with H_2O_2 (100 μmol/L, 1 hour) to induce single-strand DNA breaks yielded more striking DNA fragment tails, and these were substantially more prominent in *Nampt*-ablated SMCs. Incubation with Ang II (10^{-7} mol/L, 24 hours) yielded a modest DNA fragment signal that was significantly greater in *Nampt*-ablated SMCs (Figure 5C and 5D).

To further assess the response to DNA break–inducing agents, SMCs were tracked by video microscopy. This revealed a striking death response in *Nampt*-depleted SMCs, with cell rounding, anoikis, and cessation of cell membrane activity (Figure 5E; Online Figure VII). Incubating SMCs with methyl methanesulfonate, another single-strand DNA-breaking reagent, led to similarly worse survival for *Nampt*-ablated SMCs (Figure 5F; Online Figure VII). Notably, incubating SMCs with nicotinamide riboside before methyl methanesulfonate inhibited the death response (Figure 5G). Together, these studies reveal that Nampt protects SMCs from accumulating both oxidized DNA lesions and a toxic burden of single-strand DNA breaks.

Nampt-Deficient SMCs Have Impaired Double-Strand DNA Break Repair

Double-strand DNA breaks are a particularly stressful form of DNA damage and potent driver of cell senescence.[27] Using the above culture system, we assessed the potential for accumulating double-strand breaks by subjecting SMCs to irradiation (10 Gy) and immunostaining for phosphorylated histone (γ-H2AX). Interestingly, DNA damage foci were found in low abundance in *Nampt*-ablated SMCs before irradiation. On irradiation, damage foci accumulated and were significantly more abundant in *Nampt*-ablated SMCs. This difference was evident after 15 minutes but also after 24 hours, at which time control SMCs showed near-complete resolution of the breaks (Figure 6A and 6B). Incubation of *Nampt*-ablated SMCs with Ang II (24 hours) also increased double-strand DNA damage foci, and this effect was still evident 24 hours after Ang II washout (Online Figure VIIIa).

We next assessed whether this form of DNA damage could be found in vivo. There were no γ-H2AX–positive SMCs in the aortic media of mice subjected to vehicle infusion. Rare (<0.5%) γ-H2AX–positive cells were found in control mice subjected to Ang II infusion (Figure 6C and 6D). In contrast, γ-H2AX–positive SMCs were consistently detected in both ascending (4.0%) and descending (3.8%) thoracic aortas of Ang II–infused SMC-*Nampt* mice (Figure 6D).

PARP Activity Is Impaired in Nampt-Deficient SMCs and Its Inhibition In Vivo Promotes Aortic SMC DNA Damage and Senescence

PARP1 has roles in repairing multiple types of DNA damage.[9] To determine whether PARP1 activity was impacted by the disrupted NAD^+ metabolism, we assessed PAR assembly by Western blot analysis after irradiation of rat aortic SMCs. Irradiation-induced PAR formation was markedly suppressed in SMCs incubated with the Nampt inhibitor, FK866 (100 nmol/L; Figure 6E). The abundance of PARP1 itself did not change on Nampt inhibition. We also immunostained mouse aortic SMCs for PAR. Abundant nuclear PAR signal emerged 15 minutes after control SMCs were exposed to H_2O_2. However, there was barely detectable nuclear PAR in *Nampt*-ablated SMCs subjected to H_2O_2 (Figure 6F and 6G). In the presence of nicotinamide riboside, PAR assembly in irradiated *Nampt*-ablated SMCs was restored. Nuclear PAR also accumulated on 24 hours of Ang II exposure. As seen with H_2O_2, the Ang II–induced PAR response was not evident in *Nampt*-ablated SMCs but was restored in the presence of nicotinamide riboside (Online Figure VIIIb).

In addition, in vivo inhibition of PARP by intraperitoneal injections of olaparib produced SMC defects in control mice subjected to Ang II that were similar to those in Ang II–infused SMC-*Nampt* KO mice. The proportion of p16-expressing medial SMCs increased by 2.7-fold and 3.7-fold in the ascending and descending thoracic aorta, respectively (P=0.002; P=0.023), and the proportion of SMCs positive for 8-oxodG increased by 2.2-fold and 1.9-fold (P=0.0003; P=0.003; Online Figure IXA and IXB). As well, γ-H2AX–positive SMCs were identified in the media of Ang II–infused mice that received olaparib and in a range similar to that of Ang II–infused SMC-*Nampt* KO mice (Online Figure IXC).

Collectively, these data indicate the presence of a NAD^+–PARP1–DNA repair axis in aortic SMCs and the dependence of this cascade on Nampt.

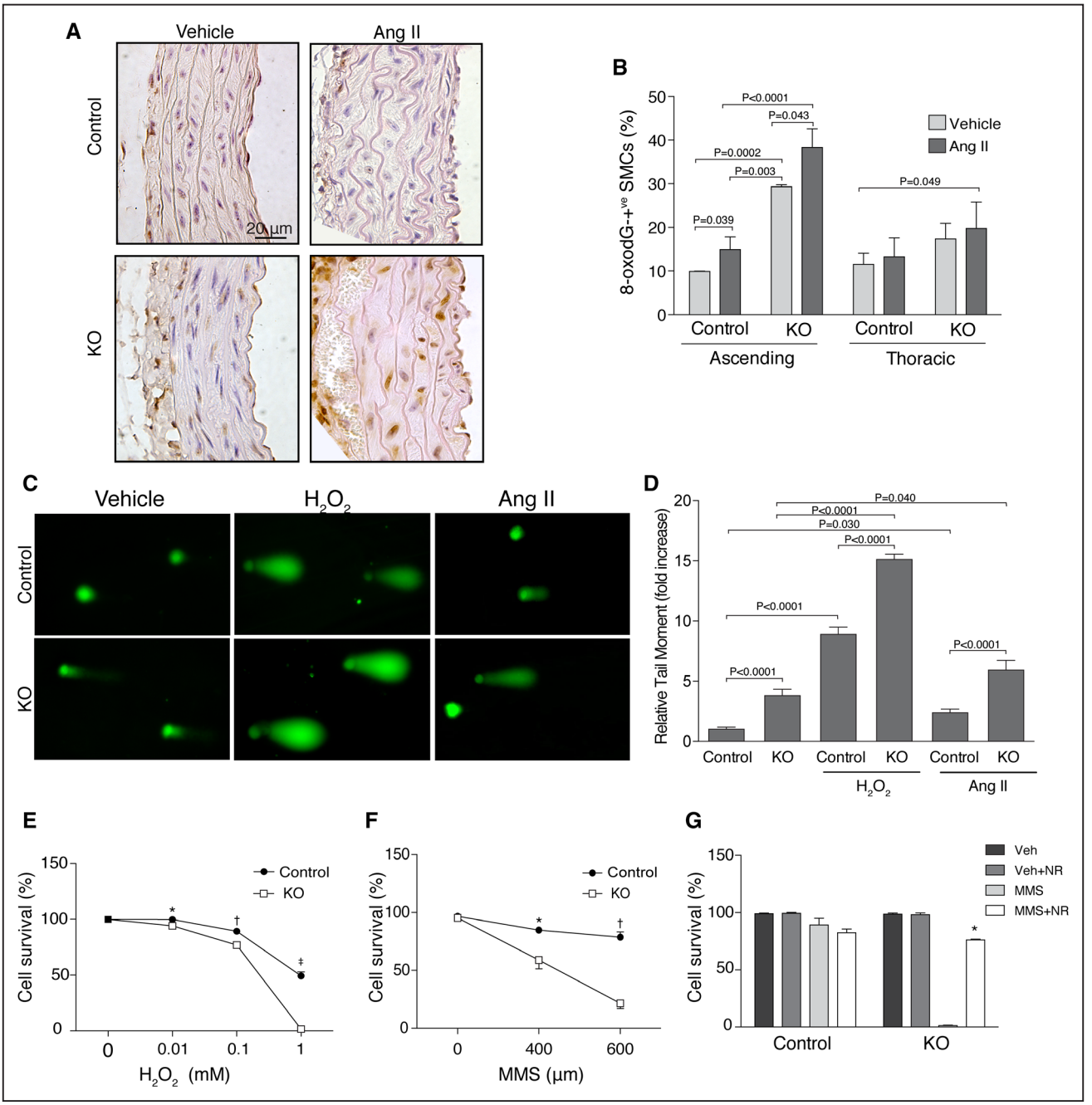

Figure 5. Nicotinamide phosphoribosyltransferase (*Nampt*) deficiency and susceptibility to oxidative DNA damage. A, Micrographs of ascending aorta 7 d after infusion with angiotensin II (Ang II), depicting oxidative DNA lesions as indicated by 8-oxo-2′-deoxyguanosine (8-oxodG) immunoreactivity. **B**, Graph showing the percentage of 8-oxodG–positive cells in the ascending and descending thoracic aortas. **C**, Fluorescent micrographs of fragmented DNA comet tails from mouse aortic smooth muscle cells (SMCs) subjected to vehicle, 100 μmol/L H_2O_2 (1 h), and 10^{-7} mol/L Ang II (24 h). **D**, Graph depicting mean±SEM SMC comet tail moments, relative to control SMCs incubated with vehicle. **P*≤0.0001. **E** and **F**, Graphs depicting survival of mouse aortic SMCs, 24 h after incubation with H_2O_2 (**P*=0.012, †*P*=0.014, ‡*P*=0.0001) or methyl methanesulfonate (MMS; **P*=0.009, †*P*<0.0001). **G**, Graph depicting the survival of mouse aortic SMCs, 24 h after incubation with 600 μmol/L MMS, with and without the addition of 100 μmol/L nicotinamide riboside (NR), **P*≤0.0001.

Media of Dilated Human Thoracic Aortas Is Populated by SMCs With DNA Strand Breaks and Low NAMPT

Given the compromised genomic integrity in the mouse models, we asked whether DNA integrity was compromised in SMCs within the human ascending aorta. This was of interest because although double-strand DNA breaks have been found in atherosclerotic lesions[28]; the media of the nonatherosclerotic aorta is considered a more quiescent vascular setting. Remarkably, γ-H2AX–immunostaining revealed that 25% of normal caliber aortas contained unrepaired DNA strand breaks in the medial layer cells. On average, 2.4% of medial cells displayed DNA damage foci (range 0–10.1%). Even more striking was that 90% of aortopathy samples had

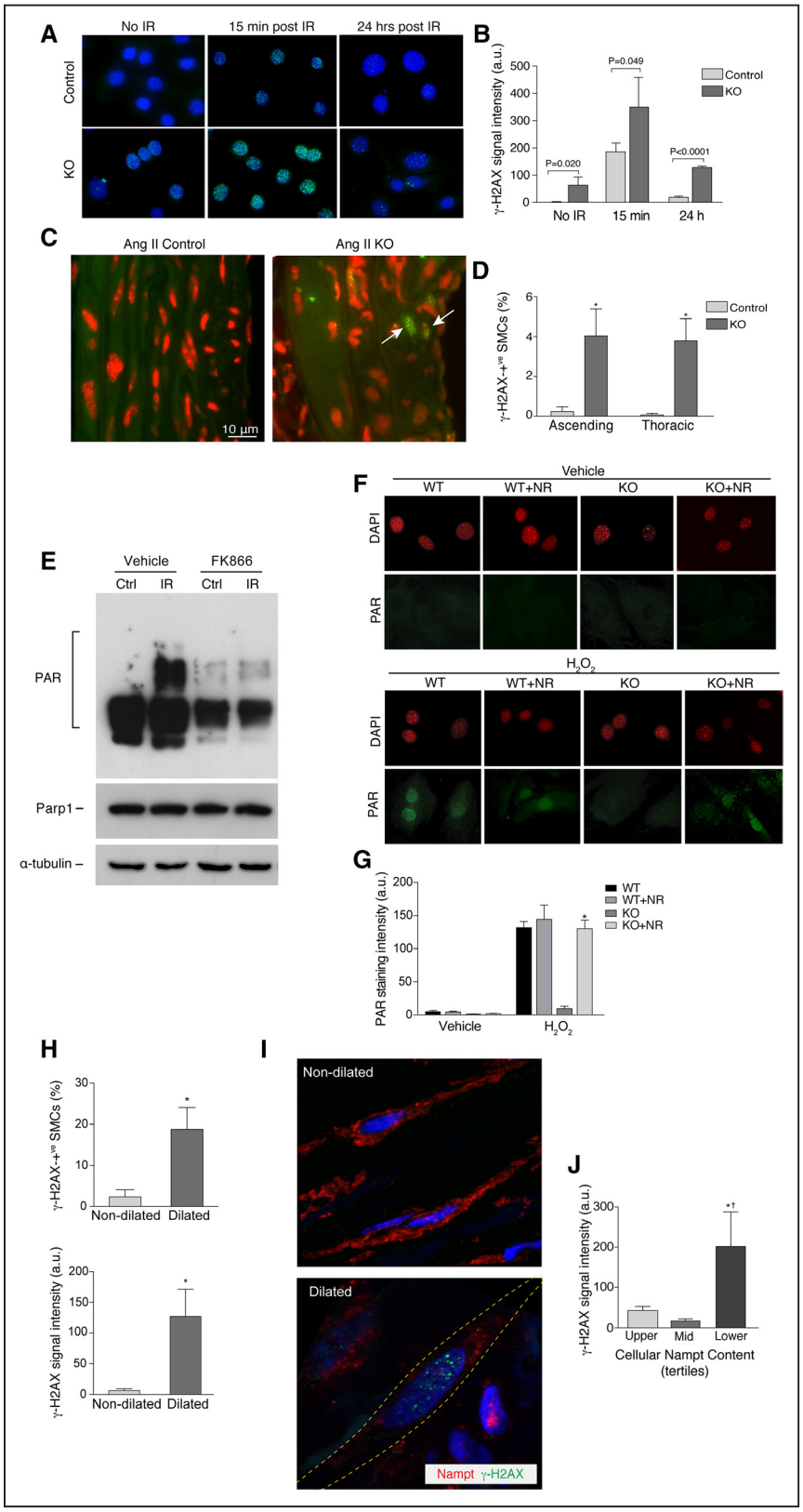

Figure 6. Reduced nicotinamide phosphoribosyltransferase (Nampt), poly(ADP-ribose) polymerase-1 (PARP1) inactivation, and double-strand DNA damage in mouse and human aortas. **A**, Fluorescent micrographs depicting the response of mouse aortic smooth muscle cells (SMCs) to irradiation (10 Gy). Cells were immunostained for γ-H2AX (green) and nuclei were labeled with Hoechst 33258 dye (blue). **B**, Graph showing the cumulative pixel intensity per cell of γ-H2AX signal. **C**, Micrographs showing γ-H2AX–positive foci (green) in nuclei in the aortic media of mice subjected to a 7-d infusion of Ang II. Nuclei were counterstained with propidium iodide (red). **D**, Graph depicting the proportion of γ-H2AX–positive cells in the aortic media of mice subjected to a 7-d infusion of angiotensin II (Ang II), **P*=0.044 vs control, ascending aorta; **P*=0.022 vs control, thoracic aorta. **E**, Western blots depicting poly(ADP-ribose) (PAR) moieties, Parp1, and tubulin content in rat aortic SMCs incubated with FK866 (24 h) and subjected to irradiation (50 Gy). **F**, Immunofluorescence images showing the presence of PAR moieties (green) in control and Nampt-knockout (KO) SMCs subjected to 1 mmol/L H_2O_2 for 15 min. Nuclei were counterstained with DAPI (4′,6-diamidino-2-phenylindole; red). **G**, Graph depicting cumulative pixel intensity per cell of PAR signal, **P*<0.0001 vs KO. **H**, Prevalence of medial SMCs in aortas with γ-H2AX signal (**top**, **P*=0.047) and intensity of γ-H2AX signal (**bottom**, **P*=0.021). **I**, Confocal photomicrographs illustrating reciprocal relationship between nicotinamide phosphoribosyltransferase (NAMPT; green) and phosphorylated histone (γ-H2AX) positivity (red) in human ascending aorta. Nuclei were counterstained with DAPI. **J**, Cellular DNA damage signal, stratified by cellular NAMPT content. **P*=0.034 vs upper NAMPT tertile, †*P*=0.013 vs mid NAMPT tertile.

evidence of unrepaired DNA strand breaks, with an average of 28.7% SMCs with DNA damage foci (range: 7.3–60.0% of cells, Figure 6H). To more precisely define the relationship between NAMPT expression and unrepaired DNA damage, we double immunolabeled aortas for NAMPT and γ-H2AX (Figure 6I). NAMPT content was then quantified in a total of 524 individual SMCs, which were separated into tertiles based on NAMPT expression. SMCs in the lowest tertile had >5-fold greater DNA damage signal than those in the mid and highest NAMPT tertiles (Figure 6J).

Hypermethylation of the NAMPT Promoter in Dilated Human Thoracic Aortas

Given the linkages between low NAMPT and DNA damage, we assessed what might underlie the low NAMPT in human thoracic aortopathy. Epigenetic control of genes relevant to aortopathy has recently been described.[29] To determine whether this might be the case for *NAMPT*, we first assessed whether the expression profile of *NAMPT* in human aortic SMCs was preserved between in vivo and culture environments. This revealed that *NAMPT* transcript abundance in early passage SMCs correlated with NAMPT abundance in the corresponding aortic media (R^2=0.72; P=0.004; Figure 7A). Furthermore, *NAMPT* transcript abundance in SMCs derived from both normal and dilated aortas was stable over 3 serial subcultures, and differences between patient SMCs were maintained (Figure 7B). Bioinformatic assessment (http://genome.ucsc.edu/) predicted a ≈1300-base CpG island surrounding the *NAMPT* transcriptional start site. Methylation analysis using selective digestion-based polymerase chain reaction revealed little to no methylation of *NAMPT* promoter DNA from nondilated human aortas. However, 13.0±4.1% of input DNA from dilated aortas was methylated (P=0.044; Figure 7C). Furthermore, in SMCs cultured from the ascending aorta, the level of promoter methylation inversely correlated with *NAMPT* mRNA abundance in the corresponding SMCs (R^2=0.028; P=0.024). This also revealed that the *NAMPT* promoter in SMCs from patients with dilated aortas was hypermethylated relative to that of SMCs cultured from control aortas (P=0.004; Figure 7D and 7E).

Discussion

This study reveals that aortic integrity depends on an intrinsic NAD^+-generating system within SMCs. By evaluating human aortopathy material and new mouse models, we demonstrate that (1) NAMPT is reduced in the aortic media of patients with aneurysmal thoracic aortic disease, (2) ablation of *Nampt* in SMCs reduces NAD^+ content in the aortic wall and renders it vulnerable to dissection, (3) Ang II sends *Nampt*-depleted SMCs in the aorta into a state of premature senescence; (4) *Nampt*-deficient SMCs are prone to accumulating a range of DNA lesions and are susceptible to exhaustion of PARP activity; (5) SMCs with low NAMPT and unrepaired DNA damage constitute a previously unrecognized SMC phenotype in human aortopathy, and (6) low NAMPT levels in human aortopathy are associated with hypermethylation of the *NAMPT* promoter.

The finding that SMC-*Nampt* KO mice have reduced aortic medial NAD^+ content is important given the multiple routes for synthesizing NAD^+. There are at least 5 dietary precursors to NAD^+, 4 of which do not require Nampt. As well, NAD^+ itself may be directly delivered to cells from nearby cellular sources, and an extracellular supply of Nampt has been characterized (eNampt).[10,13] However, the 43% drop in NAD^+ in the aortic media revealed that none of these potential

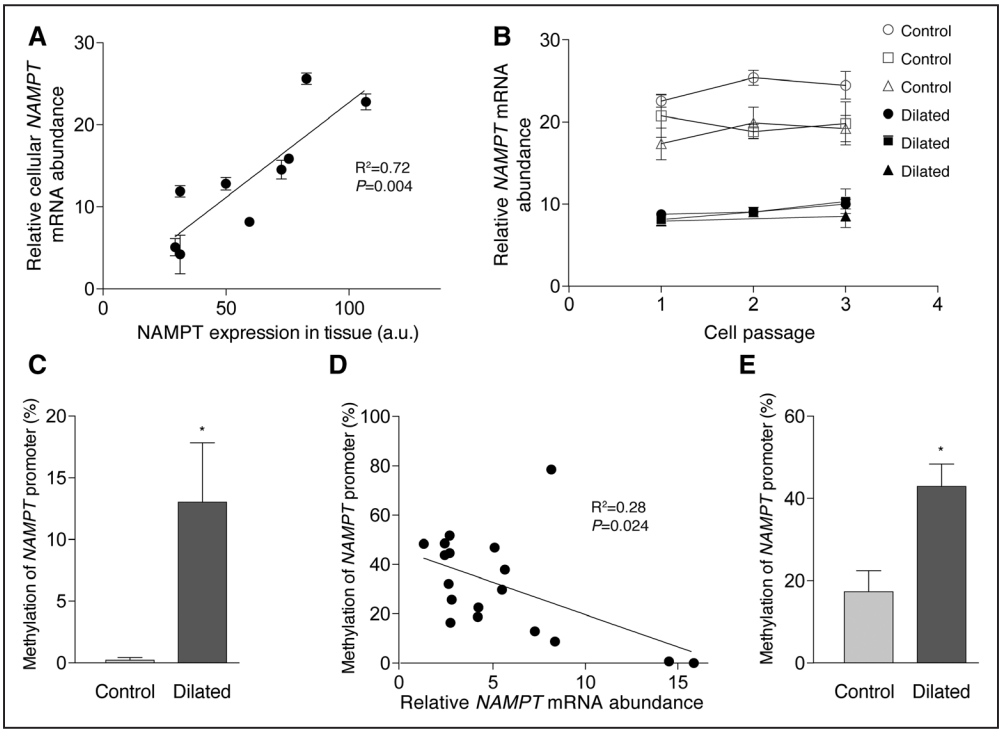

Figure 7. Hypermethylation of the nicotinamide phosphoribosyltransferase (*NAMPT*) promoter in the aortic media and cultured smooth muscle cells (SMCs) of patients with dilated ascending aortopathy. A, Relationship between *NAMPT* transcript abundance in human SMCs cultured from the ascending aorta and NAMPT content in situ in the corresponding aortic media, as assessed by immunostaining. **B**, *NAMPT* transcript abundance in early passage human SMCs derived from control and dilated patients measured over early serial cell subcultures, showing stability. **C**, Methylation of the *NAMPT* promoter in the media of control, nondilated (n=3) and dilated (n=6) aortas, **P*=0.044 vs control. **D**, Relationship between methylation of the *NAMPT* promoter in primary early passage (1–4) human SMCs and *NAMPT* transcript abundance in the respective SMCs. **E**, Methylation of the *NAMPT* promoter in early passage human SMCs derived from the ascending aorta of patients with nondilated (n=8) and dilated (n=10) aortas, **P*=0.004 vs control.

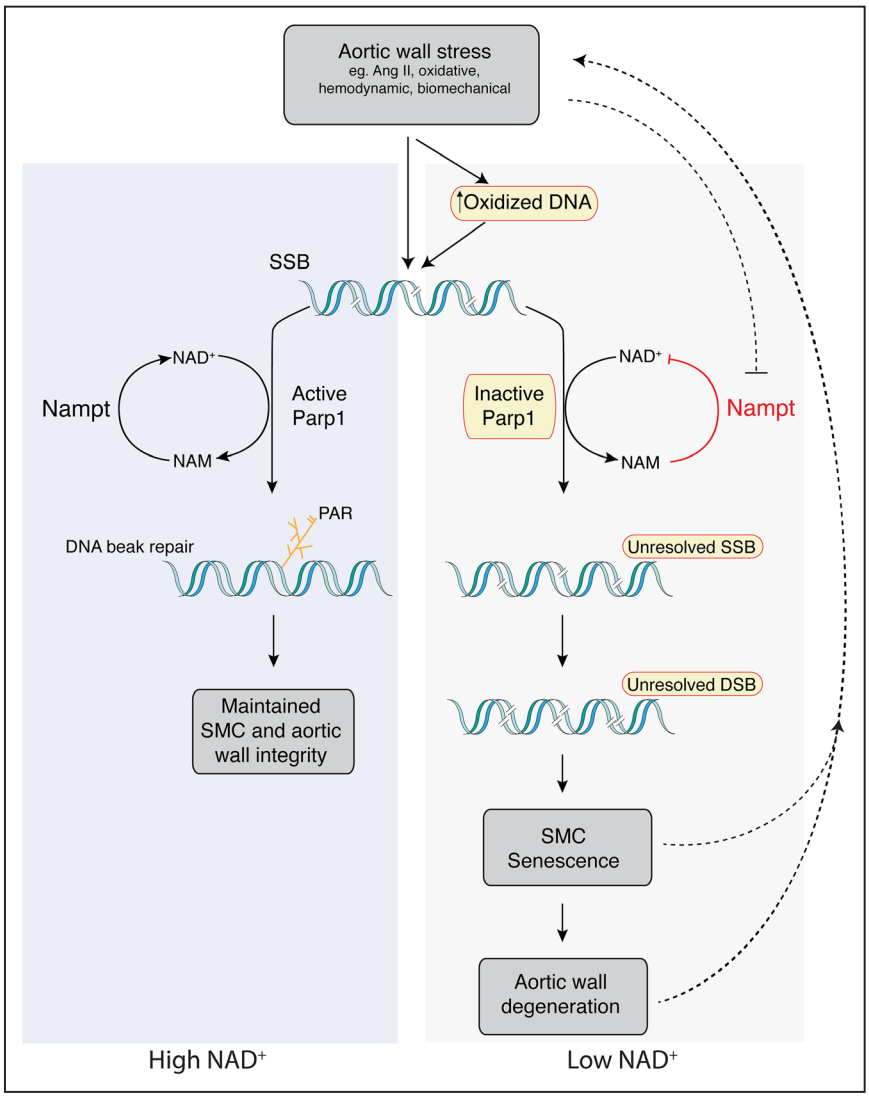

Figure 8. Schematic depicting aortic wall consequences of reduced smooth muscle cell (SMC) nicotinamide phosphoribosyltransferase (Nampt). In the setting of aortic wall insults and compromised NAD+ (**right**), SMC DNA damage accumulates and is inadequately repaired. This can lead to accelerated SMC aging and destabilization of the aortic wall. Deleterious DNA events that can be exacerbated by low Nampt are outlined in red. A proposed route to decreasing Nampt and a self-sustaining damage cycle are noted by the dashed lines. DSB indicates double-strand break; PAR, poly(ADP ribose); and SSB, single-strand break.

alternative pathways circumvented the local loss of Nampt in SMCs. Given the resulting aortic compromise and our previous studies showing no evidence for secretion of Nampt by SMCs,[12] the current data indicate that an autonomous, Nampt-dependent NAD+ production cascade in SMCs serves as a vital metabolic hub for the aorta.

The observed drop in aortic medial NAD+ was sufficient to lead to mild dilation, but more striking consequences became apparent with the stress of Ang II. Rather than adapt to this stress, the *Nampt*-deficient aortic wall degenerated, with abrogated SMC hyperplasia, overt SMC dropout, and medial hematomas and dissections. The latter had similar distributions to that of other models of aortic disruption,[23] suggesting that the reduced Nampt acted on a background of prevailing aortic susceptibilities. The additional finding of widespread SMC senescence provides an intriguing mechanistic basis for the Nampt-driven maladaptive response to Ang II. Ang II has been found to induce SMC senescence in vitro and in atherosclerotic arteries,[30,31] and the current data, thus, expand the in vivo contexts for SMC senescence. Several attributes of senescent or otherwise aged SMCs could adversely impact aortic stability including the relative inability to replicate, perturbed contractility, and an altered secretory profile that favors a pro-degeneration phenotype.[26,32]

The inability to maintain genomic integrity is a hallmark of accelerated aging and a key stimulus for cellular senescence. The range of DNA lesions that we identified place Nampt as an important guardian of genomic health. The presence of oxidized guanine residues in SMCs reflects a persistent reactive oxygen species burden that could promote senescence through several mechanisms, including lipid oxidation and interference with cellular metabolism.[26] In addition, 8-oxoguanine DNA lesions themselves have been found to be pathological, and their continuous clearance is required to prevent the cell from entering a senescence cascade.[33] Single-strand DNA breaks, readily detected in aortic SMCs depleted of *Nampt*, are also linked to cellular senescence, either directly or by predisposing to double-strand DNA breakage.[34,35] Double-strand DNA breakage in turn is a well-established driver of cellular senescence.[27] Taken together, the findings establish that compromised NAD+ constitutes an intracellular milieu that is hazardous for DNA integrity.

Although several upstream defects may contribute to the observed DNA lesions, our findings point to incapacitation

of PARP1 as an important mechanism. One of the best-understood roles of PARP1 is the sensing and repair of single-strand DNA breaks, effectively serving as the first line of defense to this common DNA assault.[9] More recent evidence has established that protein PARylation, mediated in part by PARP1, also functions in double-strand break repair.[36,37] As well, PARP1 participates in clearance of oxidized nucleotides through binding to 8-oxoguanine-DNA glycolase, an enzyme fundamental to removing 8-oxoguanine base lesions.[36,38,39] We cannot exclude the possibility that molecular perturbations arising from NAD^+ depletion other than PARP incapacitation may have contributed to aortic wall degeneration. In this regard, SIRT1 activity in SMCs has been shown to depend on a Nampt-mediated supply of NAD^+,[40] and SIRT1 has been found to protect against aortic disruption in response to Ang II.[41,42] As well, substantially reduced NAD^+ can lead to critical ATP depletion and energetic stress, which has been found to cause muscle degeneration in skeletal muscle–specific *Nampt*-knockout mice.[15] However, the threshold NAD^+ level below which ATP production becomes compromised in the aorta remains to be elucidated.

The possibility that the functional linkage between low SMC Nampt and aortic degeneration in mice translates to human aortopathy was supported by several findings. SMC NAMPT content was lower in dilated human aortas than that in nondilated aortas. Moreover, there was an inverse relationship between the aortic diameter and medial SMC NAMPT content. This fits an emerging pattern of reduced Nampt in aged or compromised tissues,[16,43] and the current study may be the first to identify such a relationship in human diseased tissue. We note that aortic medial dissection, prominent in the mouse model, was not represented in the patient series. Nonetheless, ascending aortic diameter is a strong predictor of dissection risk in patients.[44] Also remarkable was our discovery of unrepaired DNA breaks in aortic medial SMCs in situ and the relatively high prevalence of this genome pathology in the aorta of individuals with aortopathy. Although our data do not prove causation, the single-cell relationship between low NAMPT and unresolved DNA strand breaks strengthens the potential for a mechanistic relationship. Moreover, the combination of unresolved DNA breaks and low Nampt can be considered to denote a SMC phenotype of substantially declined cellular vitality.

Our findings also suggest that low Nampt may compromise the aortic response to stress independent of the primary cause of the aortopathy. Low aortic NAMPT was observed not only in the dilated aortas of patients with a bicuspid aortic valve but also in those with a tricuspid aortic valve and Marfan syndrome. A larger series would be required to determine whether there are aortic disease-specific differences in NAD^+ control and also whether NAD^+ homeostasis in SMCs is relevant to atherosclerotic abdominal aortic aneurysms.

The chronic nature of aortic dilation disease is such that a suboptimal NAD^+-regenerating system could both potentiate and sustain aortic wall degeneration. We speculate that an NAD^+ fatigue phenomenon may underlie the progression of thoracic aortopathy (Figure 8). This is supported by the finding that Ang II can reduce *Nampt* expression and NAD^+ content in the aorta and the evidence for methylation-dependent silencing of *NAMPT* expression in dilated human ascending aortas. The latter is also noteworthy because biomechanical forces are known to impact epigenetic events.[45] Thus, it is possible that aortic dilation itself might progressively repress *NAMPT* promoter activity.

In summary, we demonstrate that Nampt within SMCs protects the aorta from degenerating. Nampt fuels a critical DNA repair system in the medial aortic layer and resists premature cellular senescence. Our findings raise the possibility that disturbed local NAD^+ metabolism underlies the progression of degenerative aortic disease.

Sources of Funding

This work was supported by the Canadian Institutes of Health Research (FRN-11715, FRN-126148, and FDN-143326), the Heart and Stroke Foundation of Canada (T7081), and the University of Western Ontario (POEM). H. Yin was supported by a CIHR Fellowship.

Disclosures

None.

References

1. Schlatmann TJ, Becker AE. Histologic changes in the normal aging aorta: implications for dissecting aortic aneurysm. *Am J Cardiol*. 1977;39:13–20.
2. Howard DP, Banerjee A, Fairhead JF, Perkins J, Silver LE, Rothwell PM; Oxford Vascular Study. Population-based study of incidence and outcome of acute aortic dissection and premorbid risk factor control: 10-year results from the Oxford Vascular Study. *Circulation*. 2013;127:2031–2037. doi: 10.1161/CIRCULATIONAHA.112.000483.
3. Milewicz DM, Guo DC, Tran-Fadulu V, Lafont AL, Papke CL, Inamoto S, Kwartler CS, Pannu H. Genetic basis of thoracic aortic aneurysms and dissections: focus on smooth muscle cell contractile dysfunction. *Annu Rev Genomics Hum Genet*. 2008;9:283–302. doi: 10.1146/annurev.genom.8.080706.092303.
4. Li S, Van Den Diepstraten C, D'Souza SJ, Chan BM, Pickering JG. Vascular smooth muscle cells orchestrate the assembly of type I collagen via alpha2beta1 integrin, RhoA, and fibronectin polymerization. *Am J Pathol*. 2003;163:1045–1056.
5. Humphrey JD, Milewicz DM, Tellides G, Schwartz MA. Cell biology. Dysfunctional mechanosensing in aneurysms. *Science*. 2014;344:477–479. doi: 10.1126/science.1253026.
6. Ruiz-Torres A, Gimeno A, Melón J, Mendez L, Muñoz FJ, Macía M. Age-related loss of proliferative activity of human vascular smooth muscle cells in culture. *Mech Ageing Dev*. 1999;110:49–55.
7. van der Veer E, Ho C, O'Neil C, Barbosa N, Scott R, Cregan SP, Pickering JG. Extension of human cell lifespan by nicotinamide phosphoribosyltransferase. *J Biol Chem*. 2007;282:10841–10845. doi: 10.1074/jbc.C700018200.
8. Halushka MK, Angelini A, Bartoloni G, et al. Consensus statement on surgical pathology of the aorta from the Society for Cardiovascular Pathology and the Association For European Cardiovascular Pathology: II. Noninflammatory degenerative diseases - nomenclature and diagnostic criteria. *Cardiovasc Pathol*. 2016;25:247–257. doi: 10.1016/j.carpath.2016.03.002.
9. Dantzer F, Amé JC, Schreiber V, Nakamura J, Ménissier-de Murcia J, de Murcia G. Poly(ADP-ribose) polymerase-1 activation during DNA damage and repair. *Methods Enzymol*. 2006;409:493–510. doi: 10.1016/S0076-6879(05)09029-4.
10. Nikiforov A, Kulikova V, Ziegler M. The human NAD metabolome: functions, metabolism and compartmentalization. *Crit Rev Biochem Mol Biol*. 2015;50:284–297. doi: 10.3109/10409238.2015.1028612.
11. Cantó C, Menzies KJ, Auwerx J. NAD(+) metabolism and the control of energy homeostasis: a balancing act between mitochondria and the nucleus. *Cell Metab*. 2015;22:31–53. doi: 10.1016/j.cmet.2015.05.023.
12. van der Veer E, Nong Z, O'Neil C, Urquhart B, Freeman D, Pickering JG. Pre-B-cell colony-enhancing factor regulates NAD+-dependent protein deacetylase activity and promotes vascular smooth muscle cell maturation. *Circ Res*. 2005;97:25–34. doi: 10.1161/01.RES.0000173298.38808.27.

13. Revollo JR, Körner A, Mills KF, Satoh A, Wang T, Garten A, Dasgupta B, Sasaki Y, Wolberger C, Townsend RR, Milbrandt J, Kiess W, Imai S. Nampt/PBEF/Visfatin regulates insulin secretion in beta cells as a systemic NAD biosynthetic enzyme. *Cell Metab*. 2007;6:363–375. doi: 10.1016/j.cmet.2007.09.003.
14. Zhou CC, Yang X, Hua X, Liu J, Fan MB, Li GQ, Song J, Xu TY, Li ZY, Guan YF, Wang P, Miao CY. Hepatic NAD(+) deficiency as a therapeutic target for non-alcoholic fatty liver disease in ageing. *Br J Pharmacol*. 2016;173:2352–2368. doi: 10.1111/bph.13513.
15. Frederick DW, Loro E, Liu L, et al. Loss of NAD homeostasis leads to progressive and reversible degeneration of skeletal muscle. *Cell Metab*. 2016;24:269–282. doi: 10.1016/j.cmet.2016.07.005.
16. Stein LR, Imai S. Specific ablation of Nampt in adult neural stem cells recapitulates their functional defects during aging. *EMBO J*. 2014;33:1321–1340. doi: 10.1002/embj.201386917.
17. Yin H, van der Veer E, Frontini MJ, Thibert V, O'Neil C, Watson A, Szasz P, Chu MW, Pickering JG. Intrinsic directionality of migrating vascular smooth muscle cells is regulated by NAD(+) biosynthesis. *J Cell Sci*. 2012;125:5770–5780. doi: 10.1242/jcs.110262.
18. Wang P, Li WL, Liu JM, Miao CY. NAMPT and NAMPT-controlled NAD metabolism in vascular repair. *J Cardiovasc Pharmacol*. 2016;67:474–481. doi: 10.1097/FJC.0000000000000332.
19. Wang P, Xu TY, Guan YF, Su DF, Fan GR, Miao CY. Perivascular adipose tissue-derived visfatin is a vascular smooth muscle cell growth factor: role of nicotinamide mononucleotide. *Cardiovasc Res*. 2009;81:370–380. doi: 10.1093/cvr/cvn288.
20. de Picciotto NE, Gano LB, Johnson LC, Martens CR, Sindler AL, Mills KF, Imai S, Seals DR. Nicotinamide mononucleotide supplementation reverses vascular dysfunction and oxidative stress with aging in mice. *Aging Cell*. 2016;15:522–530. doi: 10.1111/acel.12461.
21. Rongvaux A, Galli M, Denanglaire S, Van Gool F, Drèze PL, Szpirer C, Bureau F, Andris F, Leo O. Nicotinamide phosphoribosyl transferase/pre-B cell colony-enhancing factor/visfatin is required for lymphocyte development and cellular resistance to genotoxic stress. *J Immunol*. 2008;181:4685–4695.
22. Xin HB, Deng KY, Rishniw M, Ji G, Kotlikoff MI. Smooth muscle expression of Cre recombinase and eGFP in transgenic mice. *Physiol Genomics*. 2002;10:211–215. doi: 10.1152/physiolgenomics.00054.2002.
23. Rateri DL, Davis FM, Balakrishnan A, Howatt DA, Moorleghen JJ, O'Connor WN, Charnigo R, Cassis LA, Daugherty A. Angiotensin II induces region-specific medial disruption during evolution of ascending aortic aneurysms. *Am J Pathol*. 2014;184:2586–2595. doi: 10.1016/j.ajpath.2014.05.014.
24. Owens AP 3rd, Subramanian V, Moorleghen JJ, Guo Z, McNamara CA, Cassis LA, Daugherty A. Angiotensin II induces a region-specific hyperplasia of the ascending aorta through regulation of inhibitor of differentiation 3. *Circ Res*. 2010;106:611–619. doi: 10.1161/CIRCRESAHA.109.212837.
25. Vafaie F, Yin H, O'Neil C, Nong Z, Watson A, Arpino JM, Chu MW, Wayne Holdsworth D, Gros R, Pickering JG. Collagenase-resistant collagen promotes mouse aging and vascular cell senescence. *Aging Cell*. 2014;13:121–130. doi: 10.1111/acel.12155.
26. Yin H, Pickering JG. Cellular senescence and vascular disease: novel routes to better understanding and therapy. *Can J Cardiol*. 2016;32:612–623. doi: 10.1016/j.cjca.2016.02.051.
27. d'Adda di Fagagna F. Living on a break: cellular senescence as a DNA-damage response. *Nat Rev Cancer*. 2008;8:512–522
28. Gray K, Kumar S, Figg N, Harrison J, Baker L, Mercer J, Littlewood T, Bennett M. Effects of DNA damage in smooth muscle cells in atherosclerosis. *Circ Res*. 2015;116:816–826. doi: 10.1161/CIRCRESAHA.116.304921.
29. Gomez D, Kessler K, Michel JB, Vranckx R. Modifications of chromatin dynamics control Smad2 pathway activation in aneurysmal smooth muscle cells. *Circ Res*. 2013;113:881–890. doi: 10.1161/CIRCRESAHA.113.301989.
30. Kunieda T, Minamino T, Nishi J, Tateno K, Oyama T, Katsuno T, Miyauchi H, Orimo M, Okada S, Takamura M, Nagai T, Kaneko S, Komuro I. Angiotensin II induces premature senescence of vascular smooth muscle cells and accelerates the development of atherosclerosis via a p21-dependent pathway. *Circulation*. 2006;114:953–960. doi: 10.1161/CIRCULATIONAHA.106.626606.
31. Matthews C, Gorenne I, Scott S, Figg N, Kirkpatrick P, Ritchie A, Goddard M, Bennett M. Vascular smooth muscle cells undergo telomere-based senescence in human atherosclerosis: effects of telomerase and oxidative stress. *Circ Res*. 2006;99:156–164. doi: 10.1161/01.RES.0000233315.38086.bc.
32. Liu Y, Drozdov I, Shroff R, Beltran LE, Shanahan CM. Prelamin A accelerates vascular calcification via activation of the DNA damage response and senescence-associated secretory phenotype in vascular smooth muscle cells. *Circ Res*. 2013;112:e99–109. doi: 10.1161/CIRCRESAHA.111.300543.
33. Rai P, Onder TT, Young JJ, McFaline JL, Pang B, Dedon PC, Weinberg RA. Continuous elimination of oxidized nucleotides is necessary to prevent rapid onset of cellular senescence. *Proc Natl Acad Sci USA*. 2009;106:169–174. doi: 10.1073/pnas.0809834106.
34. Nassour J, Martien S, Martin N, Deruy E, Tomellini E, Malaquin N, Bouali F, Sabatier L, Wernert N, Pinte S, Gilson E, Pourtier A, Pluquet O, Abbadie C. Defective DNA single-strand break repair is responsible for senescence and neoplastic escape of epithelial cells. *Nat Commun*. 2016;7:10399. doi: 10.1038/ncomms10399.
35. Kuzminov A. Single-strand interruptions in replicating chromosomes cause double-strand breaks. *Proc Natl Acad Sci USA*. 2001;98:8241–8246. doi: 10.1073/pnas.131009198.
36. Beck C, Robert I, Reina-San-Martin B, Schreiber V, Dantzer F. Poly(ADP-ribose) polymerases in double-strand break repair: focus on PARP1, PARP2 and PARP3. *Exp Cell Res*. 2014;329:18–25. doi: 10.1016/j.yexcr.2014.07.003.
37. Wang M, Wu W, Wu W, Rosidi B, Zhang L, Wang H, Iliakis G. PARP-1 and Ku compete for repair of DNA double strand breaks by distinct NHEJ pathways. *Nucleic Acids Res*. 2006;34:6170–6182. doi: 10.1093/nar/gkl840.
38. Noren Hooten N, Kompaniez K, Barnes J, Lohani A, Evans MK. Poly(ADP-ribose) polymerase 1 (PARP-1) binds to 8-oxoguanine-DNA glycosylase (OGG1). *J Biol Chem*. 2011;286:44679–44690. doi: 10.1074/jbc.M111.255869.
39. Fisher AE, Hochegger H, Takeda S, Caldecott KW. Poly(ADP-ribose) polymerase 1 accelerates single-strand break repair in concert with poly(ADP-ribose) glycohydrolase. *Mol Cell Biol*. 2007;27:5597–5605. doi: 10.1128/MCB.02248-06.
40. Ho C, van der Veer E, Akawi O, Pickering JG. SIRT1 markedly extends replicative lifespan if the NAD+ salvage pathway is enhanced. *FEBS Lett*. 2009;583:3081–3085. doi: 10.1016/j.febslet.2009.08.031.
41. Chen HZ, Wang F, Gao P, et al. Age-associated sirtuin 1 reduction in vascular smooth muscle links vascular senescence and inflammation to abdominal aortic aneurysm. *Circ Res*. 2016;119:1076–1088. doi: 10.1161/CIRCRESAHA.116.308895.
42. Fry JL, Shiraishi Y, Turcotte R, Yu X, Gao YZ, Akiki R, Bachschmid M, Zhang Y, Morgan KG, Cohen RA, Seta F. Vascular smooth muscle sirtuin-1 protects against aortic dissection during angiotensin II-induced hypertension. *J Am Heart Assoc*. 2015;4:e002384. doi: 10.1161/JAHA.115.002384.
43. Yoshino J, Mills KF, Yoon MJ, Imai S. Nicotinamide mononucleotide, a key NAD(+) intermediate, treats the pathophysiology of diet- and age-induced diabetes in mice. *Cell Metab*. 2011;14:528–536. doi: 10.1016/j.cmet.2011.08.014.
44. Hiratzka LF, Bakris GL, Beckman JA, *et al*; American College of Cardiology Foundation/American Heart Association Task Force on Practice Guidelines; American Association for Thoracic Surgery; American College of Radiology; American Stroke Association; Society of Cardiovascular Anesthesiologists; Society for Cardiovascular Angiography and Interventions; Society of Interventional Radiology; Society of Thoracic Surgeons; Society for Vascular Medicine. 2010 ACCF/AHA/AATS/ACR/ASA/SCA/SCAI/SIR/STS/SVM guidelines for the diagnosis and management of patients with Thoracic Aortic Disease: a report of the American College of Cardiology Foundation/American Heart Association Task Force on Practice Guidelines, American Association for Thoracic Surgery, American College of Radiology, American Stroke Association, Society of Cardiovascular Anesthesiologists, Society for Cardiovascular Angiography and Interventions, Society of Interventional Radiology, Society of Thoracic Surgeons, and Society for Vascular Medicine. *Circulation*. 2010;121:e266–e369. doi: 10.1161/CIR.0b013e3181d4739e.
45. Jiang YZ, Manduchi E, Jiménez JM, Davies PF. Endothelial epigenetics in biomechanical stress: disturbed flow-mediated epigenomic plasticity in vivo and in vitro. *Arterioscler Thromb Vasc Biol*. 2015;35:1317–1326. doi: 10.1161/ATVBAHA.115.303427.

Circulation Research
JOURNAL OF THE AMERICAN HEART ASSOCIATION

Nicotinamide Phosphoribosyltransferase in Smooth Muscle Cells Maintains Genome Integrity, Resists Aortic Medial Degeneration, and Is Suppressed in Human Thoracic Aortic Aneurysm Disease

Alanna Watson, Zengxuan Nong, Hao Yin, Caroline O'Neil, Stephanie Fox, Brittany Balint, Linrui Guo, Oberdan Leo, Michael W.A. Chu, Robert Gros and J. Geoffrey Pickering

Circ Res. 2017;120:1889-1902; originally published online March 29, 2017;
doi: 10.1161/CIRCRESAHA.116.310022
Circulation Research is published by the American Heart Association, 7272 Greenville Avenue, Dallas, TX 75231

Print ISSN: 0009-7330. Online ISSN: 1524-4571

SUPPLEMENTAL MATERIAL

Nicotinamide Phosphoribosyltransferase in Smooth Muscle Cells Maintains Genome Integrity, Resists Aortic Medial Degeneration and is Suppressed in Human Thoracic Aortic Aneurysm Disease

Detailed Methods

Generation of *Nampt*-deficient mouse models

Mouse experiments followed protocols approved by the Western University Animal Use Committee. All mice were on a C57Bl/6 background. To generate mice with a SMC-specific knockout of *Nampt*, an initial cross was undertaken between female mice harbouring loxP sites flanking exons 5 and 6 of *Nampt* (*Nampt*$^{flox/flox}$)[1] and male transgenic mice expressing Cre recombinase and eGFP under the control of the SMC-specific myosin heavy chain promoter (smMHC-Cre/eGFP, Jackson Laboratories, Bar Harbor, ME).[2] Expression of Cre in the aorta of the latter mice was verified by whole tissue epifluorescence microscopy (Zeiss SteREO Lumar V12 Microscope, Carl Zeiss Canada Ltd, Toronto, ON, Canada) and by immunostaining OCT-embedded frozen sections using an anti-eGFP antibody (Fig. S1). In a second round of breeding, the male SMC-targeted *Nampt* heterozygotes (*Nampt*$^{flox/+}$; smMHC-Cre+) were bred with female *Nampt*$^{flox/flox}$ mice. Because of transient expression of Cre in the sperm of male smMHC-Cre/eGFP mice,[3] the floxed allele transmitted from the Cre-expressing parent is recombined, yielding a global heterozygous null allele of *Nampt* (hereafter referred to as "-"). Genotyping using PCR primers to amplify floxed, wildtype, exon 5/6-deleted *Nampt*, and the Cre transgene[1, 2] confirmed the four possible genotypes of the offspring: *Nampt*$^{flox/+}$; smMHC-Cre- (wild-type), *Nampt*$^{flox/+}$; smMHC-Cre+ (SMC-specific *Nampt* heterozygous), *Nampt*$^{flox/-}$; smMHC-Cre- (global *Nampt* heterozygous), and *Nampt*$^{flox/-}$; smMHC-Cre+ (SMC-specific knockout with a global heterozygous *Nampt* background, "SMC-*Nampt* KO"). We used the wild-type mice as control and global *Nampt* heterozygous as an additional control for key endpoints. Importantly, prior studies have shown that global *Nampt* heterozygous mice are not overtly different from wild-type mice.[4] SMC-*Nampt* KO mice in the upper size tertile at 10-12 weeks of age were used for all studies.

We also generated mice in which *Nampt* could be globally and inducibly deleted. *Nampt*$^{flox/flox}$ mice were bred with mice expressing Cre recombinase fused to the mutated ligand binding domain of the human estrogen receptor (ER) under the control of a chimeric cytomegalovirus immediate-early enhancer/chicken ß-actin promoter (*B6.Cg-Tg(CAG-Cre/Esr1)5Amc/J*) (Jackson Laboratories, Bar Harbor, ME).[5] SMCs harvested from aortas of *Nampt*$^{flox/flox}$ Cre-ERT2 mice were subjected to hydroxy-tamoxifen or sunflower oil vehicle for 24 hours.

Human aorta material

Human ascending aortic tissue was obtained from patients undergoing ascending aortic replacement, coronary bypass surgery, or cardiac transplantation, as approved by the institutional review board of Western University Research Ethics Committee. Maximum aortic diameter was determined from contrast-enhanced CT scan or echocardiogram obtained prior to surgery. NAMPT levels were assessed by histology of the aortopathy material, performed on the maximally dilated region of the ascending aorta. *NAMPT* transcript abundance was assessed in human aortic medial tissue from which the adventitial and intimal layers were dissected away. RNA was isolated using TRIzol (Life Technologies) and the RNeasy Mini Kit following the manufacturer's protocol (Qiagen, Valencia, CA).

NAD^+ measurement

Mouse aortic medial NAD^+ levels were determined in freshly harvested aorta after removing the adventitial layer by dissection and denuding the endothelial layer by scraping. NAD^+ content in the mouse aortic media was determined using a colorimetric kit (BioVision Research Products, Mountain View, CA, USA) and expressed relative to total protein content.

Laser capture microdissection and RNA isolation of mouse aortas

Laser capture was undertaken on 10 μm-thick frozen sections of the mouse descending thoracic aorta that had been embedded in OCT compound (Tissue-Tek). The medial layer was micro-dissected (Arcturus 704 Veritas LCM System, Harlow Scientific, Arlington, VA) from 20 sections of an individual aorta and RNA extracted using TRIzol (Life Technologies) with the addition of linearized polyacrylamide (2 mg/ml, Sigma) following phase separation.

Drug Delivery in Mice

Mini-osmotic pumps (Alzet Model 2004, Durect Corp., Cupertino, CA) were implanted subcutaneously in the right flank for infusion with either saline or Ang II (1.44 mg/kg/day) for 7 or 28 days. Implantation was performed after inducing anesthesia with 3% isofluorane in 100% oxygen at a flow rate of 1 L/min. In a subset of mice, phenylephrine (Sigma, 30 mg/kg/day) was infused via mini-pump for 14 days, with implantation of an Ang II-infusing pump (1.44 mg/kg/day) on the opposite flank on day 7, such that both phenylephrine and Ang II were infused for seven days. PARP activity was inhibited by twice daily intraperitoneal injections of olaparib (50 mg/kg, AZD2281, Selleckchem, Houston, TX) for eight days, beginning 24 hours prior to implantation of saline or Ang II-loaded minpumps.

Blood pressure measurement

Blood pressure and heart rate were measured by noninvasive tail cuff (CODA, Kent Scientific Corp., Torrington, CT).[6] Mice were acclimatized by undergoing daily blood pressure recordings for one week prior to data acquisition. For data acquisition, 35 serial blood pressure measurements were performed and the average of the last 30 cycles recorded.

Aortic wall morphometry

Mice were anesthetized with ketamine/xylazine and perfused via the left ventricle with phosphate-buffered saline (PBS) and then paraformaldehyde (4% wt/vol) under physiological pressure for 30-45 minutes. After immersion in 4% paraformaldehyde overnight, two-mm segments from four distinct aortic zones[7] were embedded in paraffin: ascending aorta (1 mm distal to the aortic valve); descending thoracic aorta (5 mm distal to the left subclavian artery); suprarenal abdominal aorta (proximal to the superior mesenteric artery); and infrarenal abdominal aorta (distal to the left renal artery). Five-μm sections were stained with hematoxylin-eosin or Movat's pentachrome and visualized with an Olympus BX51 microscope. Medial area, lumen area, and medial cell number were quantified from 3 sections 200 μm apart, in each of the four aortic regions, avoiding areas with aortic hematoma or dissection, using ImageJ software (NIH, Bethesda, MD). Focal areas of medial cell loss in the descending thoracic region were traced and expressed relative to that of the media. Aortic dissection was defined by the presence of blood in one or more of the aortic medial layers extending contiguously for at least 200 μm.

Immunohistochemistry and apoptosis of mouse aortic tissue

Immunostaining was performed on paraffin-embedded sections (for Nampt, eGFP, 8-oxodG, smooth muscle α-actin, p16, γ-H2AX, and cascapse-3). Primary antibodies were: rabbit polyclonal anti-eGFP (AB3080 1:50; EMD Millipore, Billerica, MA), mouse monoclonal anti-smooth muscle α-actin (Clone 1A4, A5228 1:500, Sigma, Oakville, ON, Canada), rabbit polyclonal anti-Nampt (A300-372A 1:50; Bethyl Laboratory, Montgomery, TX), mouse monoclonal anti-8-oxodG (NWA-MOG020 1:50; Northwest Life Sciences, Vancouver, WA), rabbit polyclonal anti-p16 (sc-28260 1:50; Santa Cruz

Biotechnology, Dallas, TX), rabbit monoclonal anti-γ-H2AX (#9718 1:400; Cell Signaling, Danvers, MA), rabbit polyclonal anti-active caspase-3 (ab4051 1:50; Abcam, Cambridge, MA), rabbit monoclonal anti-Ki67 (ab16667 1:100; Abcam, Cambridge, MA), and rabbit polyclonal anti-CD45 (ab10558 1:200; Abcam, Cambridge, MA). Bound primary antibodies against eGFP, Nampt, 8-oxodG, p16, Ki67 and CD45 were detected using goat anti-rabbit or goat anti-mouse biotinylated antibody (Vector Labs, Burlington, ON, Canada) and visualized using an ABC kit and diaminobenzidine (DAB, Vector Labs) and counterstained with Harris' hematoxylin. Bound primary antibodies against smooth muscle α-actin and γ-H2AX were detected using Alexa Fluor 488-conjugated goat anti-mouse and donkey anti-rabbit secondary antibody, respectively (Molecular Probes; Life Technologies, Burlington, ON, Canada) and nuclei were counterstained with propidium iodide. The proportion of immuno-positive cells in a given aortic zone was ascertained from 3 sections, separated by 200 μm, with a minimum of 500 cells evaluated. Terminal deoxynucleotide transferase-mediated dUTP nick end labeling (TUNEL) was used to assess apoptosis on paraffin-embedded sections (Roche Applied Science).

Immunohistochemistry of human aortic tissue

NAMPT immunostaining was performed on paraformaldehyde-fixed, paraffin-embedded sections as above. NAMPT staining was quantified in 5 equally spaced fields of view (x40 objective) across the specimen, avoiding regions of inflammatory cell infiltration and vascularization to restrict analyses to medial SMCs. Signal was quantified using ImageJ software (NIH) with a DAB Deconvolution Plugin that separates the hematoxylin from the DAB signal. Background signal was ascertained in each tissue by capitalizing on the normal presence of interlamellar regions that do not contain SMCs. An area of at least 300 μm^2 was utilized for this. The SMC NAMPT signal was determined as the cumulative signal intensity and expressed relative to the number of nuclei in the field of view.

Sections were also double-stained for NAMPT and γ-H2AX (ab26350, 1:100; Abcam, Cambridge, MA). Bound primary antibodies were visualized with Alexa Fluor 488-conjugated donkey anti-rabbit secondary antibody and Alex Fluor 546-conjugated anti-mouse secondary antibody, respectively (Molecular Probes). Nuclei were counterstained with DAPI. NAMPT and γ-H2AX signal intensities were determined a cell-by-cell basis (total of 524 cells) using ImageJ.

Senescence associated ß-galactosidase activity

Senescence associated ß-galactosidase (SA ß-gal) activity in the mouse aortas was determined as described.[6] Briefly, anesthetized mice were subjected to antegrade perfusion via the left ventricle of phosphate-buffered saline (PBS) followed SA ß-gal solution (1 mg/ml X-Gal, 5 mmol/l potassium ferrocyanide, 5 mmol/l, potassium ferricyanide, 150 mmol/l NaCl, 2 mmol/l $MgCl_2$, 40 mmol/l citrate (titrated to pH 6.0 with NaH_2PO_4). Aortas were then harvested, incubated in SA-ßGal staining solution at 37°C for 16 h, fixed in 4% paraformaldehyde for 16 hours. Whole aortas were imaged with a Nikon SMZ800 stereomicroscope (Nikon Instruments, Mississauga, ON, Canada). Tissue was then frozen, embedded in OCT, and 10-μm cryosections were imaged microscopically to assess for positively stained blue cells.

Cell culture

Mouse aortic SMCs were isolated from aortas of 8-10-week-old mice via chemical digestion using type III porcine pancreatic elastase (250 μg/ml, Sigma) and type I collagenase (1 μg/ml, Worthington Biochemical Corporation, Lakewood, NJ).[8] SMCs were maintained in DMEM with 10% FBS and SMC identity confirmed by immunostaining for smooth muscle α-actin. Rat aortic SMCs were isolated as previously described[9] and maintained in DMEM with 10% FBS. All cells were studied within the first 4 subcultures. Human aortic SMCs were isolated by explant outgrowth as previously described [6]

Western blot analysis

Western blot analysis was undertaken with chemiluminescent detection as previously described.[10] Blots were probed by incubating with primary antibodies reacting to PAR (#528815 1:2,000; Calbiochem/EMD Millipore, Billerica, MA), PARP1 (ab6079 1:400; Abcam, Cambridge, MA), and α-tubulin (clone B-5-1-2 1:10,000, Sigma).

Detection of double-strand DNA breakage

Mouse SMCs subjected to irradiation at a dose rate of 1 Gy/minute for ten minutes (10 Gy) (Faxitron RX-650, Faxitron Bioptics, Tucson, AZ) or incubated with Ang II (10^{-7} mol/L) for 24 hours were fixed in 4% paraformaldehyde for 20 minutes. Cells were permeabilized in 0.5% Triton X-100 and incubated with rabbit antibody to γ-H2AX (#9718 1:300; Cell Signaling, Danvers, MA). Signal was detected by incubating with anti-rabbit Alexa Fluor 488 secondary antibody (Invitrogen, Burlington, ON, Canada) and nuclei were counterstained with 4′,6′-diamidino-2-phenylindole (DAPI, Invitrogen). γ-H2AX foci were quantified from at least 300 cells per condition based on fluorescent pixel density, applying a single background threshold for all images and using ImageJ, as described.[11]

Detection of global DNA strand breakage by Comet assay

Mouse SMCs incubated with 1 mM H_2O_2 (15 minutes) or 10^{-7} mol/L Ang II (24 hours) were analyzed for DNA strand breaks by single cell alkaline electrophoresis (CometAssay, Trevigen Gaithersburg, MD). Cells were trypsinized, suspended in 50 µl of low-melting point agar, transferred onto slides, and incubated at 4°C to allow the agar to set. Cells were then lysed in alkaline buffer and electrophoresed for 30 minutes with 300 mAmps of current. Cells were subsequently stained with SYBR-gold DNA stain and imaged (Olympus BX51). The comet tail moment (product of the tail length and fraction of total DNA in the tail) was measured using ImageJ and OpenComet (cometbio.org/index.html).

Time-lapse microscopy response to DNA damage

To evaluate the response to specific DNA damaging agents, *Nampt*$^{flox/flox}$ SMCs, with or without expression of CreERT2, were incubated with 1µM hydroxy-tamoxifen for 24 hours and cultured for an additional 72 hours to ensure *Nampt* depletion. Cells were incubated with designated concentrations of H_2O_2 or MMS for 1 hour and morphology tracked by video microscopy every 15 minutes for the following 24 hours. Cell death was identified based on either cell rounding with detachment from the plate, or a combination of collapse of the cytoskeleton, dissolution of nuclear structure, and complete cessation of movement. The effect of nicotinamide riboside on MMS-induced DNA damage was assessed by pre-incubating cells with 100 µM nicotinamide riboside (Chromadex, Irvine, CA) for 24 hours in NAD^+ precursor-free modified Eagle's medium (MEM) prior to addition of 600 µM MMS.

Immunocytochemical detection of poly(ADP-ribose)

Mouse SMCs fixed in 4% paraformaldehyde were permeabilized in 0.5% Triton X-100 and incubated with mouse anti-PAR antibody (4335-MC-100, 1:500; Trevigen, Gaithersburg, MD). PAR signal was detected with Alexa Fluor 546-conjugated goat anti-mouse secondary antibody (Molecular Probes; Life Technologies, Burlington, ON, Canada) and nuclei were counterstained with DAPI. PAR signal was quantified from at least 300 cells per condition based on fluorescent pixel density, applying a single background threshold for all images and using ImageJ, as described.[11]

Quantitative real-time reverse transcription–polymerase chain reaction

Total RNA was isolated from homogenates of the mouse aorta using TRIzol (Life Technologies) and the RNeasy Mini Kit following the manufacturer's protocol (Qiagen, Valencia, CA). Total RNA was isolated from mouse and human SMCs using the RNeasy Mini Kit following the manufacturer's protocol. Transcript abundance of *Nampt* and *Gapdh* in microdissected mouse aortas was assessed using TaqMan chemistry-based primer-probe sets (Nampt, Mm00451938_m1; Gapdh, Mm99999915_g1, Applied

Biosystems). Transcript abundance of mouse *Nampt*, *Acta2*, *Mmp2*, *Col1a1*, *Timp1*, and 18S, and human *NAMPT* and 18S, were assessed using SYBR-green chemistry-based primer sets (mouse *Nampt:* F-GGCACCACTAATCATCAGACCTG R-AAGGTGGCAGCAACTTGTAGCC; mouse *Acta2*: F-TGCTGACAGAGGCACCACTGAA R-CAGTTGTACGTCCAGAGGCATAG; mouse *Mmp2*: F-GAGACCATGCAGTCAGCTCTAG R-TAGAGCTGCCTCTTGTCTGGT; mouse *Col1a1:* F-CCTCAGGGTATTGCTGGACAAC R-CAGAAGGACCTTGTTTGCCAGG; mouse *Timp1:* F-TCTTGGTTCCCTGGCGTACTCT R-GTGAGTGTCACTCTCCAGTTTGC; mouse 18S F-GTAACCCGTTGAACCCCATT R-CCATCCAATCGGTAGTAGCG; human *NAMPT* F-AGGGTTACAAGTTGCTGCCACC R-CTCCACCAGAACCGAAGGCAAT; human 18S F-ACCCGTTGAACCCCATTCGTGA R-GCCTCACTAAACCATCCAATCGG). Quantitative real-time RT-PCR was performed using an ABI Prism (model 7900HT) and Sequence Detection System software (Life Technologies; Applied Biosystems). For mouse aortas and SMCs, relative mRNA abundance was quantified based on critical threshold (CT) using the comparative CT formula, $2^{-\Delta\Delta CT}$, with *Gapdh* or 18S mRNA as an internal control. For human aortic medial tissue and human primary SMCs, mRNA abundance was quantified based on the standard curve method, with 18S mRNA as an internal reference control, and expressed as relative units (r.u.)

Analysis of DNA methylation

Human aortic media was isolated by laser capture microdissection of 10 μm-thick frozen sections. Genomic DNA was harvested from this tissue and from cultured human SMCs using the DNeasy Blood and Tissue Kit (Qiagen). DNA was subjected to selective digestion-based PCR to quantify methylation status using the Epitect Methyl DNA Restriction Kit (Qiagen) and the pre-designed Epitect qPCR Methyl Promoter Primer set (335002 EPHS113392-1A). The amount of input DNA that was methylated was determined using the manufacturer-supplied algorithm.

Statistical analyses

Values are expressed as mean±standard error of the mean. Statistical analyses were performed using GraphPad Prism software (GraphPad, La Jolla, CA, USA). Mean data were compared using Student's t-test or one- or two-way ANOVA with Holm-Sidak *post hoc* testing. The prevalence of aortic dissection and of in vivo SA ß-gal activity were compared among groups by chi-squared analyses. The relationship between NAMPT content and human aortic dilatation was determined using linear regression analysis (SPSS, IBM Corp. Armonk, NY). To assess the single-cell relationship between NAMPT and γ-H2AX signal, within-patient cellular NAMPT content was segregated into tertiles.

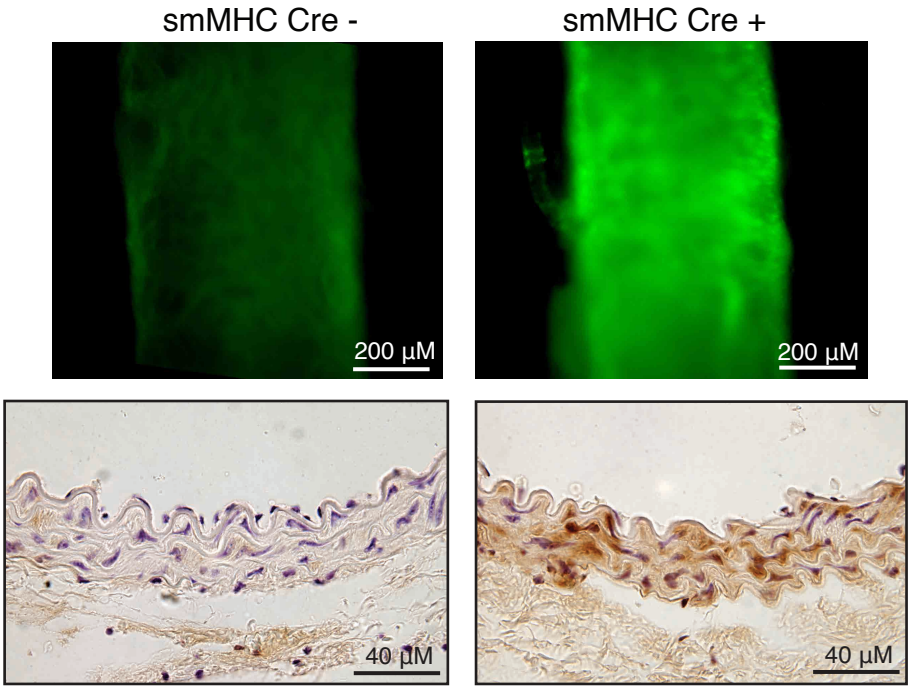

Online Figure I eGFP expression in aorta of smMHC-Cre-eGFP+ mice

Fluorescent stereomicroscopy images of whole thoracic aortas (top) and immunostained paraformaldehyde-fixed sections of thoracic aorta (bottom), depicting eGFP signal in 8-week-old smMHC-Cre-eGFP+ mice.

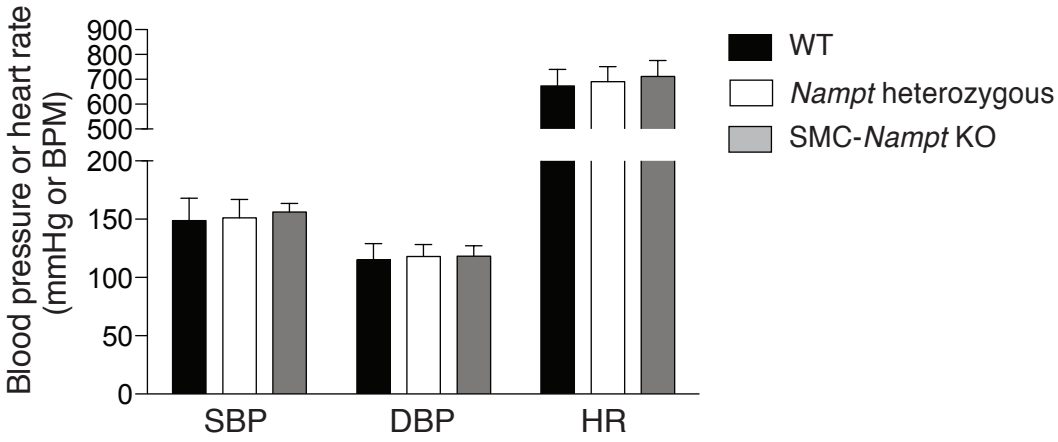

Online Figure II Blood pressure and heart rate of wild-type, *Nampt* heterozygous, and SMC-*Nampt* knockout mice

Measurements were obtained weekly for 6 weeks for each mouse and averaged. Values depict mean data from 10-12 mice per genotype.

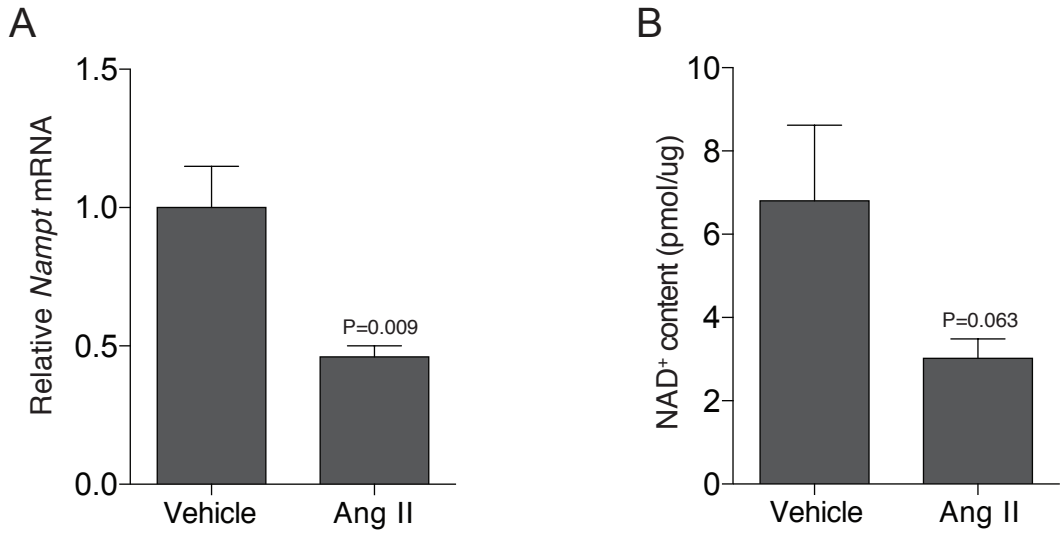

Online Figure III Angiotensin II decreases *Nampt* expression and NAD^+ content in mouse aortas.

A. Graph depicting *Nampt* transcript abundance in the media of the thoracic aorta of C57Bl/6 mice infused with Ang II (1.44mg/kg/day) or vehicle for 7 days, measured by quantitative RT-PCR. (n=3 mice per group) **B.** Graph of NAD^+ content in acidic extracts of aortic media of vehicle- or Ang II-infused mice (n=4 mice per group).

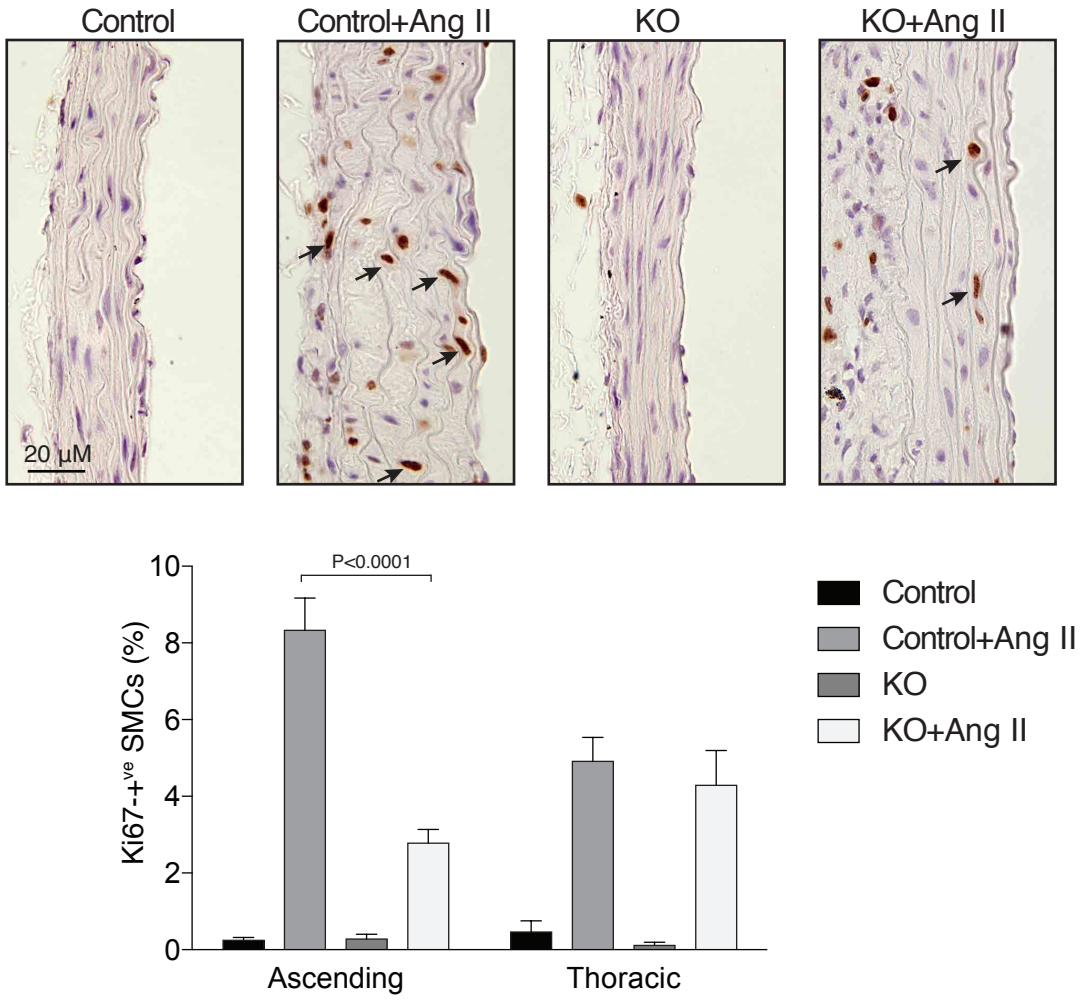

Online Figure IV Mouse aortic medial SMC proliferation as determined by immunostaining for Ki67

Micrographs of sections of the ascending aorta from control and SMC-*Nampt* KO mice after 7-day infusions of vehicle or Ang II (1.44 mg/kg/day), immunostained for Ki-67 (arrows). Quantitative data for both ascending and descending thoracic aorta sections are shown in the graph. Ang II increased Ki67-positivity ($p<0.0001$) in both control and SMC-*Nampt* KO mice, although the latter was blunted in the ascending aorta.

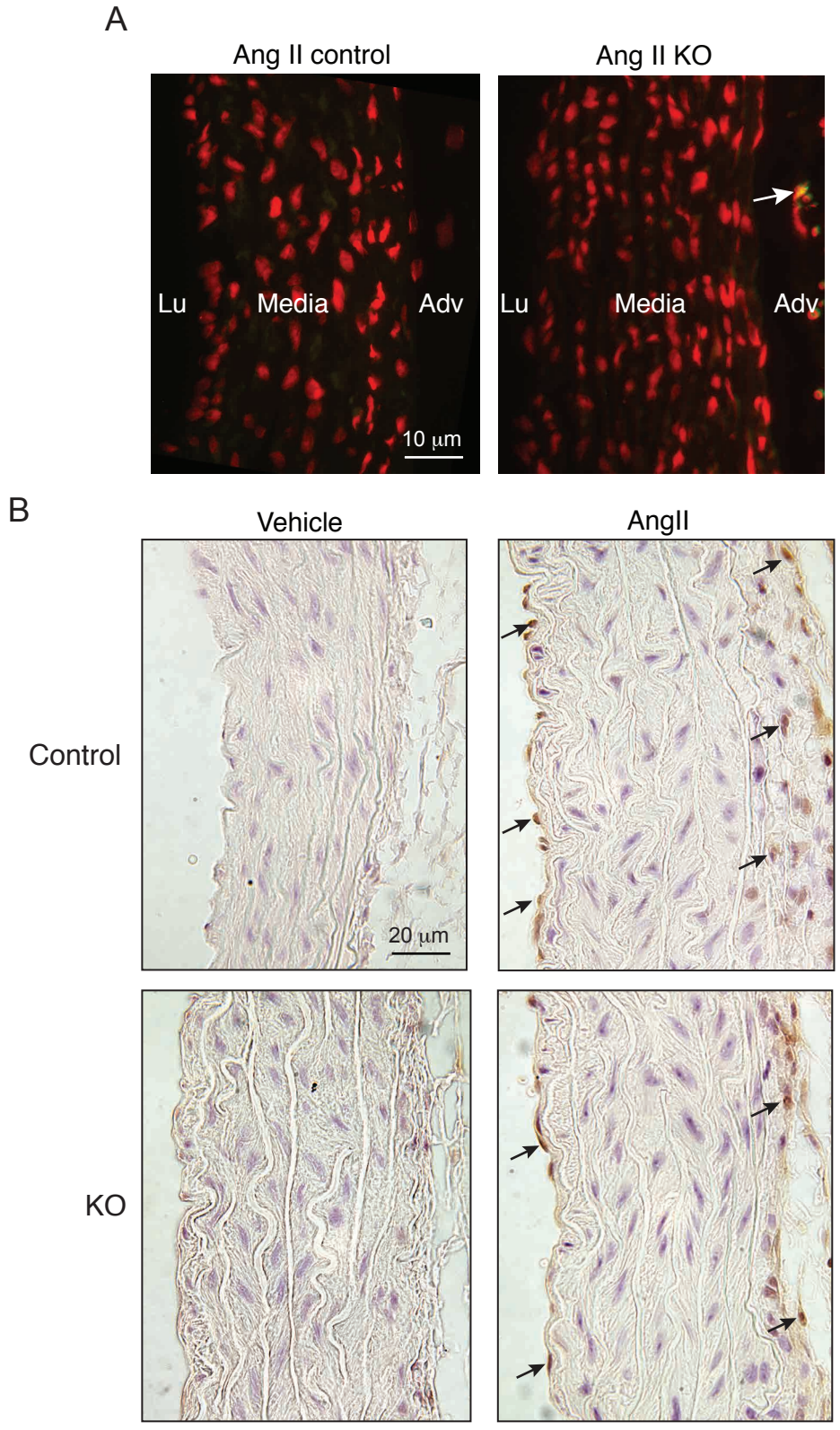

Online Figure V Assessment of apoptosis in aortas by TUNEL and active caspase-3 expression

A. Fluorescent photomicrographs of ascending aorta of mice infused with Ang II for 7 days stained using TUNEL (green). Nuclei were counter-stained with propidium iodide (red). Arrow indicates a TUNEL-positive nucleus in the adventitia. Lu, lumen; Adv, adventitia **B.** Ascending aorta sections of mice infused with vehicle or Ang II for 7 days and immunostained for active caspase-3 and counterstained with hematoxylin. Arrows indicate active caspase-3-positive endothelial cell and adventitial cell nuclei.

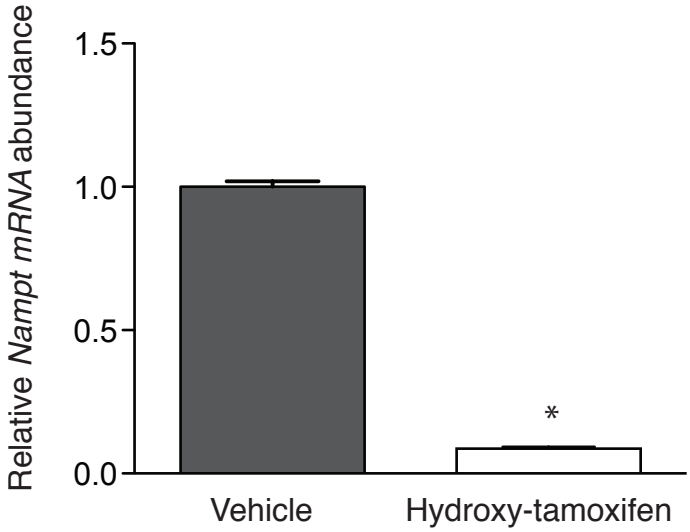

Online Figure VI Conditional deletion of *Nampt* in mouse aortic smooth muscle cells

SMCs were harvested and cultured from aortas of *Nampt*$^{flox/flox}$; CreERT2+ mice and incubated with vehicle or hydroxy-tamoxifen for 24 hours. Abundance of *Nampt* mRNA was evaluated by RT q-PCR and normalized to expression of *Gapdh* mRNA. *P<0.0001

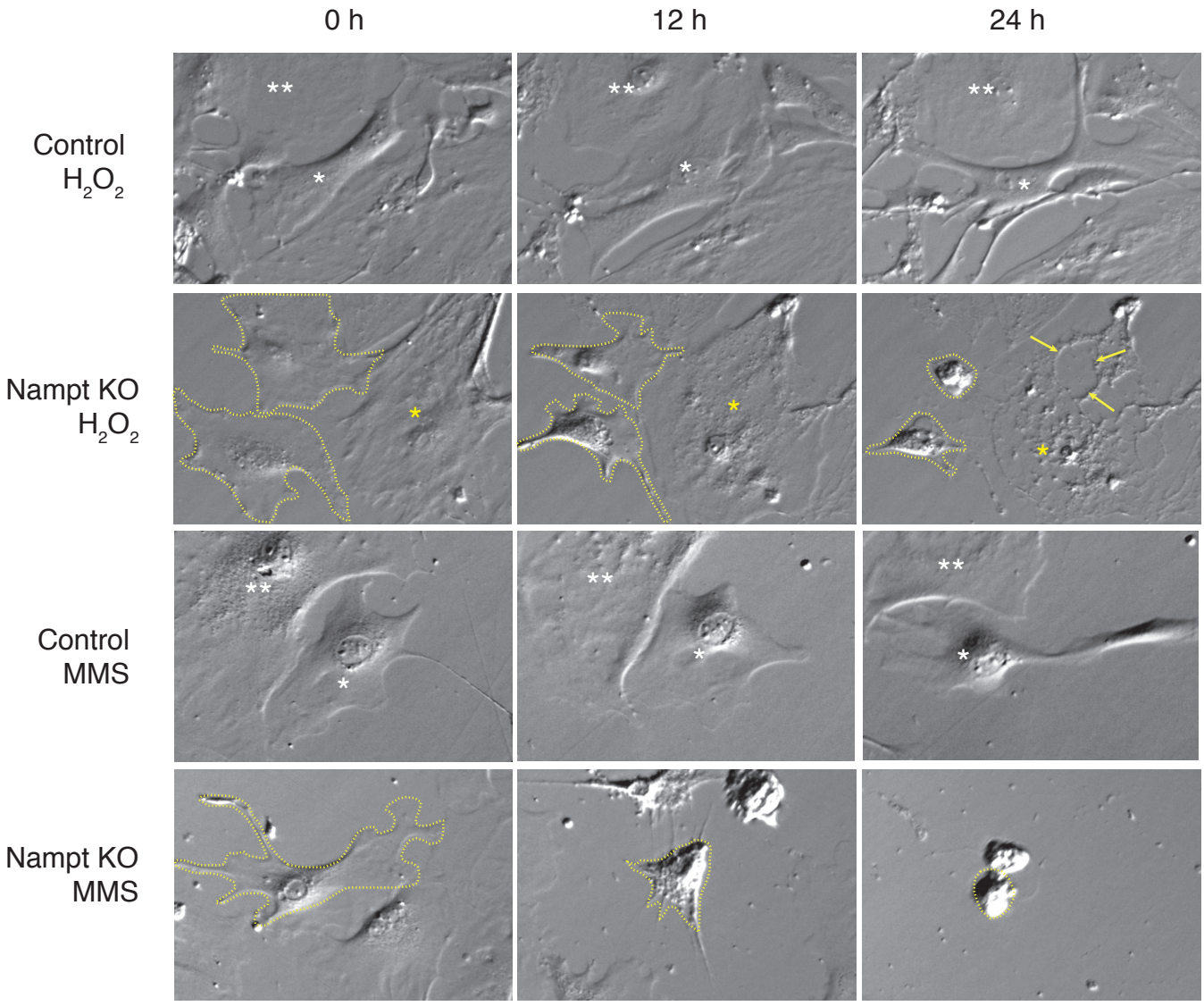

Online Figure VII ***Nampt*-depleted mouse SMCs are susceptible to death following exposure to H_2O_2 and methyl methanesulfonate.**

Time-lapse video images of control (vehicle-treated) and *Nampt*-depleted (hydroxy-tamoxifen-treated) aortic SMCs harvested from *Nampt*$^{flox/flox}$; CreERT2+ mice. SMCs were incubated for one hour with H_2O_2 (1 mM), methyl methanesulfonate (MMS, 600 μM), or respective vehicles, and tracked for 24 hours. Asterisks and cell tracings depict individual cells over the 24 h time course, with tracings denoting cells undergoing anoikis. Arrows depict a zone of cell content disintegration.

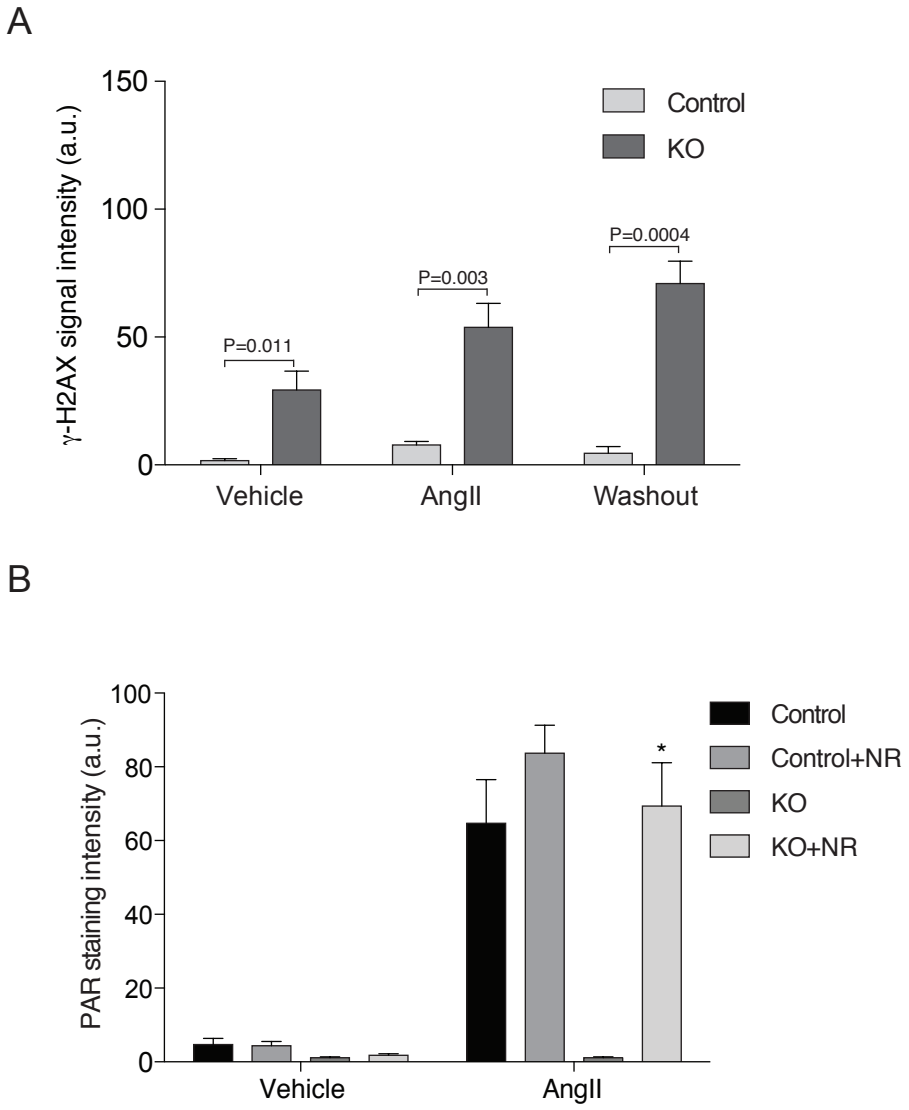

Online Figure VIII Effect of *Nampt* deficiency on Ang II-induced DNA damage and PARP1 activation in mouse aortic SMCs

A. γ-H2AX signal in control and *Nampt*-ablated mouse aortic SMCs incubated with vehicle or 10^{-7}M Ang II for 24 hours, and 24 hours after Ang II washout. **B.** Nuclear PAR signal, assessed by immunofluoresence, in mouse aortic SMCs subjected to 10^{-7}M Ang II for 24 hours, with and without the addition of 100 μM nicotinamide riboside (NR) **P*<0.0001 vs. KO.

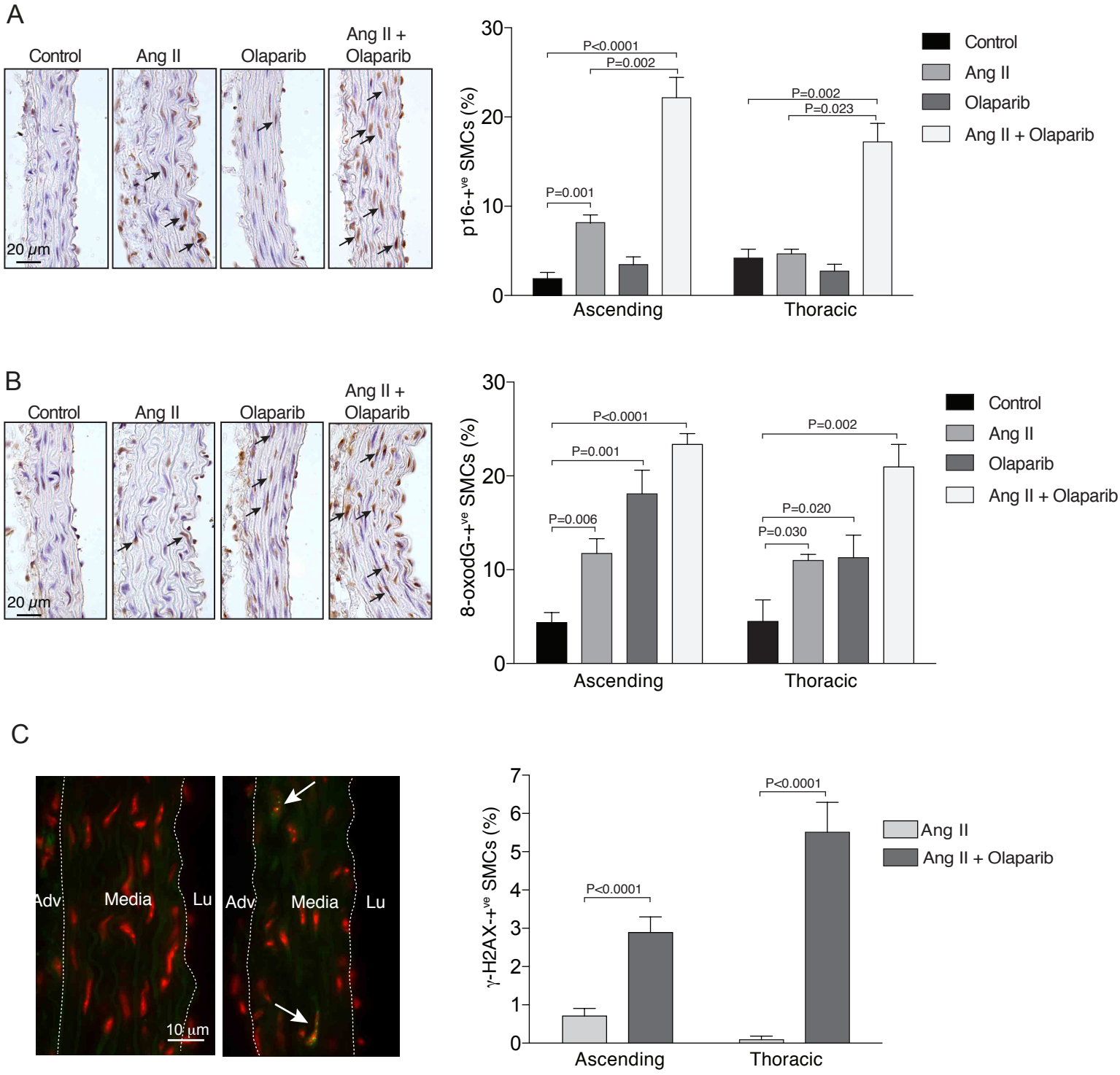

Online Figure IX Effect of PARP inhibition on aortic SMC senescence and susceptibility to oxidative DNA damage

A. Micrographs of ascending aorta sections 7 days after infusion with Ang II (1.44 mg/kg/day) as well as daily i.p. injections of the PARP inhibitor, olaparib (50 mg/kg). Sections were immunostained for p16 (arrows). Graph depicting the prevalence of p16-positive nuclei in the ascending and descending thoracic aorta is shown on the right. **B.** Sections of ascending aorta depicting oxidative DNA lesions, as indicated by 8-oxo-2'-deoxyguanosine (8-oxodG) immunoreactivity. Graph on the right depicts the abundance of 8-oxodG-positive SMCs. **C.** Micrographs showing γ-H2AX-positive foci (green) in nuclei in the aortic media of mice subjected to Ang II infusion and PARP inhibition with olaparib. Nuclei were counterstained with DAPI (pseudocolored red). Lu, lumen; Adv, adentitia. Data on the right depict the proportion of γ-H2AX-positive cells in the ascending and descending thoracic aortic media.

Online Table I. Demographic and clinical characteristics of study subjects

Age	Sex	Aortic valve configuration	Aortic Valve Dysfunction	Maximum diameter of ascending aorta (mm)
64	Female	Bicuspid	Severe AR	54
82	Male	Tricuspid	Moderate AR	57
37	Male	Bicuspid	None	57
44	Male	Bicuspid	Severe AR	68
73	Male	Bicuspid	Moderate AR/AS	55
55	Male	Tricuspid	Severe AR*	77
59	Male	Bicuspid	Severe AS	42
40	Male	Bicuspid	Severe AR/AS	57
64	Male	Bicuspid	Severe AS	43
80	Female	Tricuspid	Moderate AR	56
79	Male	Bicuspid	None	56
75	Female	Tricuspid	None	63
52	Male	Bicuspid	Moderate AR	61
56	Male	Bicuspid	None	53
32	Male	Bicuspid	Severe AR	40
62	Male	Tricuspid	Moderate AR	60
61	Male	Bicuspid	Severe AS	43
49	Female	Bicuspid	Severe AS	41
30	Female	Tricuspid	Mild AR*	50
75	Male	Bicuspid	Moderate AR	54
83	Male	Tricuspid	None (CAD)	35
53	Male	Tricuspid	None (CAD)	30
85	Female	Tricuspid	None (CAD)	33
ND	ND	ND	None (Transplant donor)	ND
70	Female	Tricuspid	None (Transplant recipient)	24
39	Female	Tricuspid	None (Transplant recipient)	29
70	Male	Tricuspid	None (CAD)	34
78	Male	Tricuspid	None (CAD)	32
79	Female	Tricuspid	Moderate AS	28
86	Female	Tricuspid	None (CAD)	33
78	Male	Tricuspid	None (Mitral valve insufficiency)	31
50	Male	Tricuspid	None (CAD)	31
68	Female	Tricuspid	None (CAD)	29
72	Male	Tricuspid	None (CAD)	32
66	Male	Tricuspid	None (CAD)	34
54	Male	Tricuspid	None (CAD)	32

***Marfan syndrome; AR-Aortic Regurgitation; AS-Aortic Stenosis; CAD-coronary artery disease**

Online Table II. Angiotensin II-induced aortic medial hemorrhage in mice

	WT		***Nampt* Heterozygous**		**SMC-*Nampt* KO**	
	Ang II (7 days) (*n=17*)	Ang II (28 days) (*n=10*)	Ang II (7 days) (*n=7*)	Ang II (28 days) (*n=7*)	Ang II (7 days) * (*n=14*)	Ang II (28 days) † (*n=8*)
Ascending	4 (23%)	0	1 (14%)	1 (14%)	6 (43%)	1 (13%)
Thoracic	0	0	0	0	1 (7%)	1 (13%)
Suprarenal	0	0	0	0	2 (14%)	4 (50%)
Infrarenal	0	0	0	0	0	0
Total (all regions)	4 (5.9%)	0	1 (3.6%)	1 (3.6%)	9 (16%)	6 (18.7%)
Total (all mice)	4 (23%)	0	1 (14%)	1 (14%)	7 (50%)	5 (62.5%)

**P*=0.0002 vs 7-day WT, *P*=0.0068 vs 7-day *Nampt* Heterozygous
†*P*=0.0106 vs. 28-day WT, *P*=0.0328 vs 28-day *Nampt* Heterozygous

References

1. Rongvaux A, Shea RJ, Mulks MH, Gigot D, Urbain J, Leo O, Andris F. Pre-b-cell colony-enhancing factor, whose expression is up-regulated in activated lymphocytes, is a nicotinamide phosphoribosyltransferase, a cytosolic enzyme involved in nad biosynthesis. *Eur J Immunol*. 2002;32:3225-3234
2. Xin HB, Deng KY, Rishniw M, Ji G, Kotlikoff MI. Smooth muscle expression of cre recombinase and eGFP in transgenic mice. *Physiol Genomics*. 2002;10:211-215
3. de Lange WJ, Halabi CM, Beyer AM, Sigmund CD. Germ line activation of the Tie2 and SMMHC promoters causes noncell-specific deletion of floxed alleles. *Physiol Genomics*. 2008;35:1-4
4. Revollo JR, Korner A, Mills KF, Satoh A, Wang T, Garten A, Dasgupta B, Sasaki Y, Wolberger C, Townsend RR, Milbrandt J, Kiess W, Imai S. Nampt/Pbef/Visfatin regulates insulin secretion in beta cells as a systemic nad biosynthetic enzyme. *Cell Metab*. 2007;6:363-375
5. Hayashi S, McMahon AP. Efficient recombination in diverse tissues by a tamoxifen-inducible form of cre: A tool for temporally regulated gene activation/inactivation in the mouse. *Dev Biol*. 2002;244:305-318
6. Vafaie F, Yin H, O'Neil C, Nong Z, Watson A, Arpino JM, Chu MW, Wayne Holdsworth D, Gros R, Pickering JG. Collagenase-resistant collagen promotes mouse aging and vascular cell senescence. *Aging Cell*. 2014;13:121-130
7. Owens AP, 3rd, Subramanian V, Moorleghen JJ, Guo Z, McNamara CA, Cassis LA, Daugherty A. Angiotensin II induces a region-specific hyperplasia of the ascending aorta through regulation of inhibitor of differentiation 3. *Circ Res*. 2010;106:611-619
8. Ray JL, Leach R, Herbert JM, Benson M. Isolation of vascular smooth muscle cells from a single murine aorta. *Methods Cell Sci*. 2001;23:185-188
9. Small TW, Pickering JG. Nuclear degradation of Wilms' Tumor 1-associating protein and survivin splice variant switching underlie IGF-1-mediated survival. *J Biol Chem*. 2009;284:24684-24695
10. Frontini MJ, O'Neil C, Sawyez C, Chan BM, Huff MW, Pickering JG. Lipid incorporation inhibits Src-dependent assembly of fibronectin and type I collagen by vascular smooth muscle cells. *Circ Res*. 2009;104:832-841
11. Fell VL, Schild-Poulter C. Ku regulates signaling to DNA damage response pathways through the Ku70 von willebrand a domain. *Mol Cell Biol*. 2012;32:76-87